FLOATFARM
NEXT GENERATION FLOATING WIND FARMS

DELIVERABLE D1.1

Novel generator design and performance

Liselotte Ulvgård[1]
Anders Hagnestål[1]
Johan Åström[1]
Irene Giuliani[2]
Francesco Papi[2]
Alessandro Bianchini[2]

[1] Hagnesia Wind AB, Hindås Sweden
Email:l liselotte.ulvgard@hagnesia.com

[2] Department of Industrial Engineering, Università degli Studi di Firenze, Florence
E-mail: fr.papi@unifi.it

June 2025

Document track information

Project information	
Project acronym	FLOATFARM
Project title	Developing the next generation of environmentally friendly floating wind farms with innovative technologies and sustainable solutions
Starting date	01/01/2024
Duration	48 months
Programme	HORIZON EUROPE
Call identifier	HORIZON-CL5-2023-D3-01
Grant Agreement No	101136091

Deliverable information	
Deliverable number	1.1
Work package number	1
Deliverable title	Novel generator design and performance
Lead beneficiary	Hagnesia
Authors	Liselotte Ulvgård, Anders Hagnestål, Johan Åström, Irene Giuliani, Francesco Papi, Alessandro Bianchini
Due date	30.06.2025
Actual submission date	30.06.2025
Type of deliverable	Report
Dissemination level	Public

Funded by the European Union

Views and opinions expressed are however those of the author(s) only and do not necessarily reflect those of the European Union or the European Climate, Infrastructure and Environment Executive Agency (CINEA). Neither the European Union nor CINEA can be held responsible for them.

Revision table

Version	Contributors	Date	Description
V0.0	Hagnesia & UNIFI	16/05/2025	First Draft
V1.0	Hagnesia & UNIFI	12/06/2025	Final Draft
V2.0	UNIFI	26/06/2025	Final version after internal review

List of acronyms

Acronym	Full name
BEM	Blade Element Momentum Method
CAD	Computer Aided Design
CAPEX	CAPital Expenditure
DD	Direct Drive
DEL	Damage Equivalent Load
EU	European Union
FEA	Finite Element Analysis
FOWT	Floating Offshore Wind Turbine
IEA	International Energy Agency
MDAO	Open Multidisciplinary Design Analysis and Optimization
NREL	National Renewable Energy Laboratory
NSS	Normal Sea State
OPEX	OPErational Expenditure
PM	Permanent Magnet
PMSG	Permanent Magnet Synchronous Generator
PTF	Poloidal or Tangential Flux
REE	Rare Earth Elements
RNA	Rotor Nacelle Assembly
RWT	Reference Wind Turbine
SSS	Severe Sea State
TRL	Technology Readiness Level
VRPM	Variable Reluctance Permanent magnet
WEIS	Wind Energy with Integrated Servo-control
WP	Work Package

About FLOATFARM

The FLOATFARM project is a Research and Innovation Action funded by the European Union under the Horizon Europe program. This project is closely linked to the FLOATECH project (2020-2023) and aims to bring the technologies developed within FLOATECH to the next level of technological readiness, complementing them with a significant number of new concepts, innovations and methods.

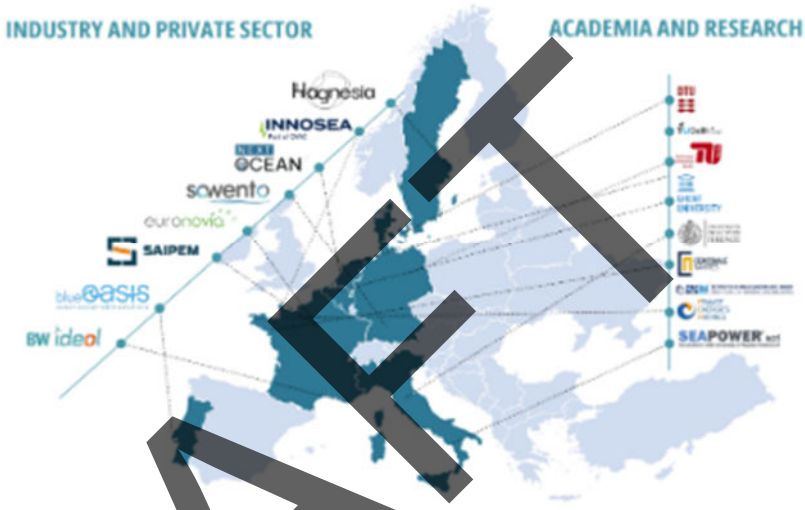

FLOATFARM aims to significantly advance the maturity and competitiveness of floating offshore wind (FOW) technology by increasing energy production, achieving significant cost reductions within the design and implementation phases, improving offshore wind value chain and supporting EU companies in this growing sector. Additionally, FLOATFARM aims to decrease negative environmental impacts on marine life and to enhance the public acceptability of FOW, thereby accelerating the EU energy transition.

The FLOATFARM consortium is coordinated by the Technische Universität Berlin and is made up of 17 partners spread across 8 countries, each contributing to technology and scientific excellence in the wind energy sector.

The approach of FLOATFARM can be broken down into three actions:

1) **Turbine Technology**: Development of innovative technologies and methods for improvements on an individual FOW turbine level,

2) **Farm Technology**: Development, investigation and demonstration of technologies that are applicable to an array of turbines within a FOW farm,

3) **Environmental & Socioeconomic Impacts**: Model development, data collection and scenario analysis of environmental, economic and sociological impacts of FOW farms.

Table of contents

Executive Summary

This document is a deliverable of the FLOATFARM project, founded by the European Union under grant agreement No 101136091.

In Work Package 1 (WP1), the FLOATFARM project aims to advance innovative technologies specifically tailored for Floating Offshore Wind Turbines (FOWTs), with the goal of improving overall performance, reducing material usage, and ultimately lowering the Levelized Cost of Energy (LCOE). The developments focus on rotor aerodynamics, drivetrain dynamics, and control systems, with particular attention to the benefits enabled by their coupling. WP1 will explore the potential of low specific power rotors to enhance energy capture in floating conditions. It will also advance a novel, lightweight, gearless generator technology developed by the partner Hagnesia and will explore its potential in new FOWT design, quantifying its potential benefits in terms of load reduction and turbine dynamics.

As a matter of fact, in Floating Offshore Wind Turbines (FOWTs), the generator weight is a critical factor. Placed several hundred meters above sea level, this component can induce significant gravitational and inertial loads on the tower and substructure as the floating platform moves and tilts. In particular, this report focuses specifically on the work carried out within Task 1.2 dedicated to the generator. The scope was to demonstrate the possible benefits in terms of FOWT design disclosed by the new generator technology. The analyses were aimed at investigating potential tower redesign strategies able to allow material saving and loads reduction at tower base and in the substructure. First, a methodology for redesigning the tower is presented, which starts from the design proposed for the IEA 15 MW Reference Wind Turbine (RWT), with the IEA-developed generator being replaced by an equivalent design using Hagnesia's generator. Building on their novel direct drive generator technology, Hagnesia has developed and evaluated different possible design configurations for a drop-in-replacement of the IEA 15 MW RWT. By developing and comparing key design and performance characteristics for different possible design solutions, two generator suggestions are selected to evaluate system level impact through turbine impact studies. Based on these suggested redesigns, an assessment was made of the potential weight and load reduction achievable through this technology. Aero-servo-hydro elastic simulations are conducted to evaluate the impact of this technology on reducing structural loads. For this analysis, the met-ocean conditions derived from a European site in the H2020 project FLOATECH are utilized. The analysis showed that Hagnesia technology can reduce generator mass by over 90% — from 270 t to approximately 20 t — while increasing conversion efficiency by around 1%. This significant reduction in nacelle weight allows for a redesigned tower, cutting its mass by 30% (approximately 400 t). As a result, redesigning just the generator and tower—excluding additional expected savings in the nacelle and platform—can enable total material savings of around 650 t. These savings also include several critical raw materials, such as copper and rare-earth elements.

1. Introduction

Nacelle weight plays an important role in Floating Offshore Wind Turbine (FOWT) design. This component is cantilevered hundreds of meters above sea level and can introduce significant inertial and gravitational loading on the tower and substructure as the turbine tilts and moves. As explained in more detail in the following sections, offshore wind turbines often use gearless generators. While the absence of a gearbox increases availability and reduces maintenance, gearless generators are often heavy, adding significant weight to the nacelle. As a consequence of the heavy nacelle and the movement of the FOWT, structural loads are generally higher than in bottom-fixed or onshore applications, and towers need to be appropriately built to resist them.

In addition, FOWT towers are typically designed conservatively to meet frequency and stiffness requirements, aiming to avoid critical excitation frequencies such as the rotational speed (1P) and blade-passing (3P) frequencies. This approach results in heavier towers compared to their onshore counterparts, leading to higher capital expenditures, increased raw material usage, and greater gravitational and inertial loads on the tower base and substructure. In this context, Task 1.2 within Work Package 1 (WP1) of the FLOATFARM project aims to evaluate potential structural load reductions and raw material savings enabled by the development of lightweight, gearless generator technology. This technology is designed to reduce the nacelle weight and, consequently, the structural loads acting on the tower and substructure. The newly developed drop-in replacement for the direct-drive generator in the IEA 15 MW Reference Wind Turbine, designed by Hagnesia, achieves a tenfold reduction in generator mass, located at the top of the tower. This significant mass reduction leads to a decrease in the loads experienced by both the tower and the substructure. The decrease in buckling constraints and stress that the tower must withstand is a key enabler for these material savings. The adoption of this technology offers multiple benefits. In floating offshore wind systems, system dynamics play a critical role, as platform motion significantly increases structural loads and displacements. Therefore, reducing material usage not only lowers capital costs but also alleviates overall system loading.

The report addresses the potential impact that the novel generator technology from Hagnesia could have on wind turbine design, focusing on the generator and its impact on tower design. For generator design, the report will provide background to the generator technology and the available design choices when upscaling it to a 15 MW design. By introducing a modular way of rescaling design and performance characteristics of numerically and experimentally validated building blocks, a sweep of different possible design configurations is presented. Based on this, two specific designs are nominated for further turbine studies. Regarding the turbine impact studies, the aim of this report is twofold. First, it proposes a redesign of the wind turbine tower subjected to a reduced generator mass thanks to the gearless direct-drive Hagnesia generator. This is achieved using the recently developed Wind Energy with Integrated Servo-control (WEIS) framework [1] coupled with QBlade [2]. This first phase results in a significant reduction in tower mass (approximately 30%) and leads to considerable material savings. Second, a comprehensive structural load analysis is performed to quantify the actual reduction in loads and to evaluate the advantages of implementing a lighter generator on the overall system performance. Load alleviation on the tower and substructure is achievable by reducing both the tower and generator mass.

1.1. Technology trends and challenges for offshore wind turbine drivetrains

Looking at wind power drive train technologies, the onshore market is dominated by gearbox solutions while the offshore wind industry is favoring direct drive (no gearbox) solutions, mainly due to high costs related to maintenance. Direct drive (DD) can be implemented in various ways, where Permanent Magnet (PM) Synchronous Generators (SG) using a radial flux topology are typically used. These DD-PMSG benefit from superior availability (lower maintenance need) and high efficiency, which is especially important for offshore applications, where they hold 75% of the global market share [3]. Important drawbacks are their capital expenditure (CAPEX) costs, weight and that they are reliant on big quantities of critical raw materials, such as Rare Earth Elements (REEs) used in the generator magnets. Alongside a considerable environmental impact, this also introduces geopolitical supply chain risk and rising costs due to an accelerated demand from a variety of clean energy technologies. REEs are listed as both strategic and critical raw materials in the EU and are highlighted as the most critical material for wind power.

Looking at the prospects for upscaling, which will be key to achieving techno-economic feasibility for large offshore power production, the generator size scaling is already a bottleneck. Ruled by the physical scaling principles that all conventional electrical machines tend to have in common, an increase in turbine power rating will lead to an even larger increase in size and weight of the DD generator. Figure 1 shows the results from two NREL studies, addressing generator weight as a function of rated power [4]. This challenge with drivetrain upscaling is a critical roadblock for enabling the next generation of offshore wind. Especially for floating wind, as the tower and floater must be designed to withstand the wind- and wave induced loads of a heavier rotor-nacelle-assembly (RNA).

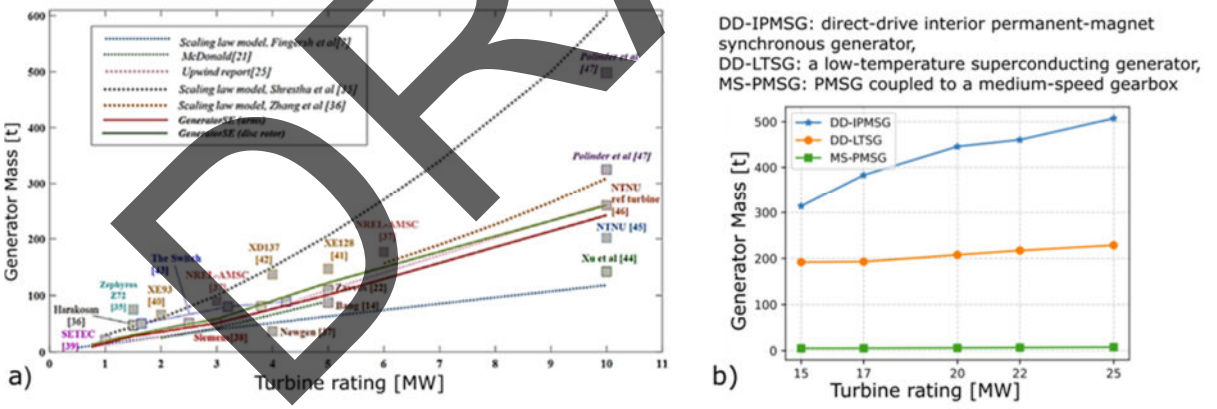

Figure 1 Weight scaling of direct drive generators. *a) PM DD generator mass for turbines rated between 0.75 and 10 MW, according to GeneratorSE model (red line) vs. existing designs* [4]*. b) Generator mass for turbine ratings 15-25 MW, based on a more recent NREL* study*. The blue line represents a conventional radial flux generator using reduced-dysprosium magnets, while the orange line represents a novel low-temperature superconducting generator. The green line is stated as a medium speed generator (using a 1:120 gearbox which is not included in the weight)*

Understanding the challenge and limitations of upscaling wind power generators

The size, and thus cost, of generators is dimensioned by the torque that they are able to achieve. All conventional generators have relatively low torque density, meaning they require more material to

generate torque compared to gearboxes. The state-of-the-art gearboxes today have a torque density of around 200 Nm/kg, while the typical torque density of a direct drive generator is around 50 Nm/kg.

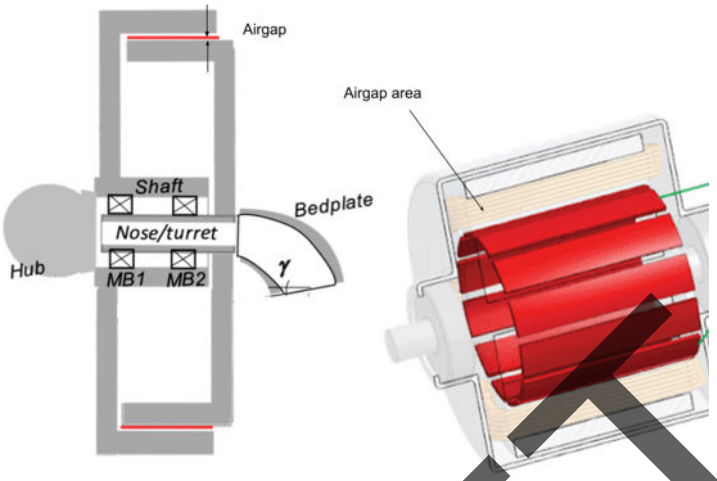

Figure 2 Illustration of a conventional radial flux direct drive generator as part of the wind power nacelle, highlighting the airgap area in red.

Generators can still achieve high power density when operating at high speeds (power = torque × speed). This is why gearboxes are used to gear up the rotational speed of the primary mover to RPMs that fit a more compact generator operating at higher speed. Considering the extremely low speed (thus high torque) that wind power operates at (which only grows more extreme when upscaling the turbine), the torque, size and weight of the gearbox is also a challenge.

While gearboxes transfer power mechanically, generators transfer the mechanical torque from the prime mover via electromagnetic forces in the airgap between stator and rotor, see Figure 2. The achievable torque is limited by the airgap area between stator and rotor as well as the magnetic shear stress achieved in the airgap, typically around 40–100 kN/m². Considering this, the minimum achievable size and weight of the generator is inherently limited by:

1. **Active material requirements:** To generate the needed shear stress, a certain amount of active materials (steel laminations, copper, and possibly magnets) is required. This results in a minimum thickness of rotor and stator, limiting how much force can be produced per kilogram. A larger airgap will require more active material to maintain a certain shear stress.
2. **Structural material requirements:** The strong magnetic forces between rotor and stator must be structurally supported across the machine. While overall symmetry balances these forces globally, local structures still need to carry them, requiring stiffness to maintain the airgap.
3. **The airgap area:** In order to increase the rated torque of the generator, a larger airgap area must be achieved, which is typically done by increasing diameter and length. However, scaling up the size of the machine will also require larger airgaps due to thermal expansion, mechanical tolerances, and structural stiffness concerns. A rule of thumb: 1 mm airgap per meter of rotor diameter (e.g., 10 mm for a 10-meter rotor). A larger airgap will require more active material to generate the needed shear stress, which will generate additional structural material (item 1+2).

These limitations lead to increasing generator weight when upscaling turbines, as seen in Figure 1. As a consequence, this contributes to increased structural weight, and costs, in other components of the turbine. To reduce the mass and cost, and to increase efficiency of the direct drive generators, several other novel generator concepts have been investigated and demonstrated:

- The axial flux synchronous generator is an old invention that electromagnetically is similar to a conventional radial flux machine. By having the airgap arranged in axial planes instead of radial cylinders, they can achieve shorter flux paths on average and also less structure material, which would result in a lighter generator. There are, however, also challenges with this topology. They are mainly related to manufacturing the parts, achieving sufficiently good tolerances at the airgap and providing enough mechanical stiffness to counteract the magnetic attraction forces and maintain the airgap. Earlier, the Belgian company Magnax [5] had ambitions in this technology. Another company that pursues this path now is the UK company Greenspur [6].

- Variable reluctance permanent magnet machines (VRPM), which implement flux switching/magnetic gearing (not the same as magnetic gears). This machine family includes transverse flux machines (TFM), flux switching machines, Vernier hybrids, modulated pole machines etc. The most explored variant for wind power is the TFM, where ring-shaped DD generators have been suggested [7]. While managing to reduce losses at low speeds, they suffer from other severe problems (including but not limited to complex design & manufacturing, low power factor, cogging and vibrations [8]) which have stopped them from being commercialised.

- Machines with integrated magnetic gears, such as the pseudo direct drive by the UK company Magnomatics [9]. The machine has a quite complex construction but has a predicted efficiency of 98-99% [10] which is very high. Also, the mass and size are significantly reduced compared to a PMSG DD although more PMs are used.

- Superconducting machines: By using superconducting materials to reduce electrical resistance, these generators can achieve greater efficiency and reduce the need for rare earth materials. In the Ecoswing project [11], a 3.6 MW machine was constructed and tested. Results show a 40% reduction in mass compared to conventional generators. A drawback is the system complexity including the cryostat that cools the superconductors.

Figure 1b shows the results from a recent NREL study of how generator weight scales with rated power in the 15-25 MW range, including both a conventional radial flux direct drive generator (using a more lightweight version of the IEA reference turbines) as well as a superconducting generator design.

1.2. The Hagnesia wind power generator

The Swedish start-up Hagnesia develops the PTF (Poloidal or Tangential Flux) technology, which specialises in low-speed DD applications. Its novel electromagnetic topology enables exceptionally

high torque density (and thus superior material efficiency), as well as an improved conversion efficiency (and thereby increased energy production) for low-speed drivetrain applications. This makes it particularly attractive for wind power, where it has a disruptive potential to enhance the competitiveness and sustainability of existing renewable energy technologies—while also enabling entirely new ones.

As further detailed in the following background section, the key characteristics of the Hagnesia generator technology are:

- **A massive weight reduction** (approximately 90% at megawatt scale), in both active materials (electrical steel, copper, and permanent magnets) and structural components. This will also enable significant structural material savings in the entire wind turbine, as further studies within the scope of this report.
- **Improved drivetrain efficiency.** Compared to conventional DD generators, which typically achieve 94–96% electrical efficiency, while the Hagnesia concept could reach 98–99%.
- **Enhanced sustainability**, addressing all three dimensions:
    - **Economic** – through substantial material savings and higher efficiency, which reduce CAPEX and increase energy yield.
    - **Environmental** – via the lower material demand and higher efficiency, resulting in a markedly reduced environmental footprint for the entire wind turbine[1].
    - **Social** – by reducing dependence on critical raw materials—including both light and heavy rare-earth elements (neodymium and dysprosium) as well as copper for windings—while strengthening Europe's technological competitiveness in wind power.

Background – understanding the innovation

The Hagnesia PTF generator technology is built from conventional materials but with an innovative electromagnetic design which enables very thin magnetic structures, allowing multiple stator and rotor disks to be stacked together, while retaining a very high force (magnetic shear stress) in the airgap. This is combined with an innovative mechanical design that provides structural stability to these thin structures so that the necessary airgap distance can be maintained. The result is an extremely torque dense machine, where much more force-producing airgap area can be accommodated per unit volume as illustrated in Figure 3. The topology also enables shorter and thicker windings, which grossly lowers resistive losses, thus giving a higher efficiency. If compared to transverse flux machines, which have similarities, it should also be noted that the PTF-design does not suffer the same low power factor and complex iron construction with 3D magnetic paths.

[1] *Regarding environmental impact, a previous life cycle assessment (LCA) of the Hagnesia generator used in the IEA 15 MW reference turbine found that climate change contributions over a 20-year time horizon could be reduced by 92% at the generator level and by 16% at the turbine level* [12]. *This study included raw material extraction, manufacturing, transport, and installation, but excluded operation and end-of-life stages. It also used more conservative assumptions for material savings in the tower.*

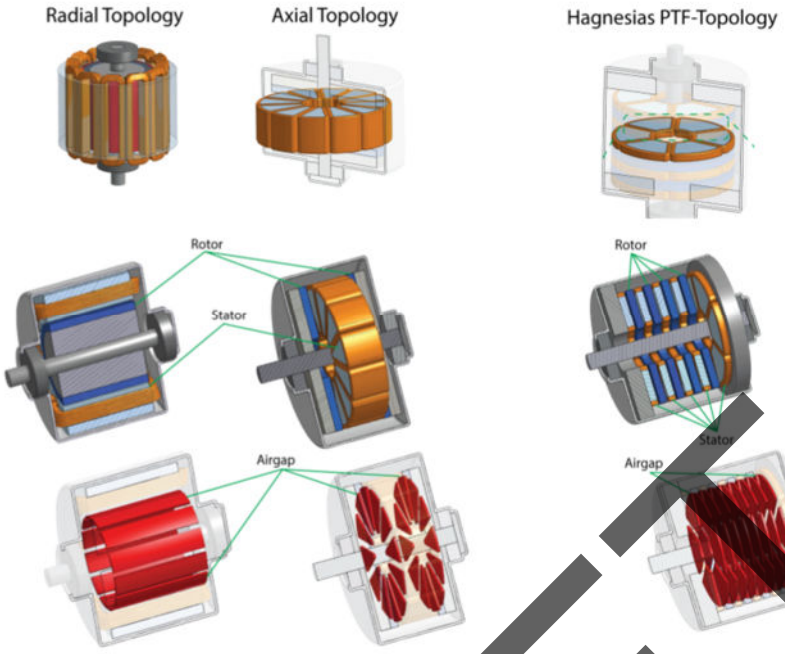

Figure 3 Comparison of Hagnesia's PTF topology compared to conventional radial and axial flux topologies, highlighting its capability to accommodate much more airgap area (in red).

The technology is protected by six patent families [13] [14] [15] [16], either granted or pending. It is currently at Technology Readiness Level (TRL) 4, where a small-scale prototype has been built and tested on a laboratory test bench. Additional prototypes are under design and construction, targeting both motor and generator applications. These prototypes are mainly intended to validate more advanced manufacturing processes and demonstrate the scalability of the technology through the integration of multiple disks. This will help confirm both the overall design integrity, performance and scale-up potential.

As part of the project NextGen [17], a downscaled prototype of a 10 MW wind power generator is being developed and tested in 2026. This prototype will deliver a torque of ~80 kNm and it will be tested across a wide speed range, up to 75 RPM (corresponding to 600 kW) in order to map and validate performance at relevant airgap speeds (which will also correlate to relevant electrical frequencies).

Drivetrain integration & design space

Figure 4 provides a schematic comparison between the Hagnesia generator and a conventional radial flux DD generator for wind turbines. The red areas illustrate the airgap between the stator and rotor. As illustrated, the Hagnesia topology enables an axial flux design that allows for compact stacking of multiple torque-producing airgaps. Based on the geometry and placement of the Hagnesia generator, several key characteristics can be highlighted:

- The Hagnesia generator consists of narrow stator and rotor disks (with airgaps in-between), stacked between two endcaps that form the generator's yoke. The current design employs an inner rotor configuration.
- Compared to conventional DD generators, the Hagnesia design is more compact in both diameter and axial length, and overall thinner than state-of-the-art machines. Combined

with its extensive weight reduction, this compactness may open opportunities for drivetrain improvements in other parts of the nacelle—though these aspects are beyond the scope of this report.

- The torque output (and thus rated power) can be scaled in two primary ways: by increasing the machine radius (thereby enlarging the airgap area per disk pair), or by adding additional disk pairs. Notably, adding disks increases the generator length only incrementally. Neither the endcaps nor the radial depth of the generator will change significantly during upscaling.
- Unlike conventional radial flux machines, the Hagnesia generator employs an axial flux architecture. This means that magnetic normal forces and tolerance chains are decoupled from the drivetrain. While the generator still requires tight tolerances and precise dynamic load control, these requirements are confined within the generator itself, reducing mechanical complexity at the turbine system level.

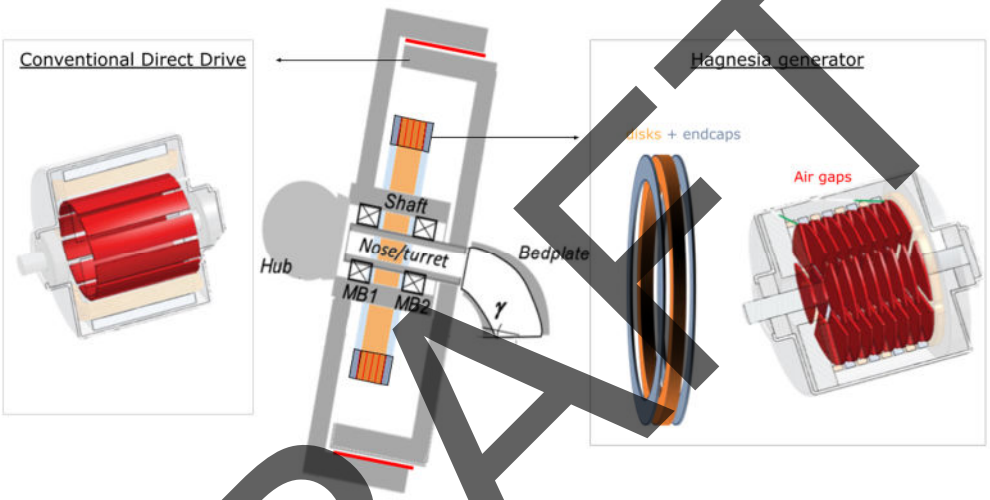

Figure 4 Topology comparison of the Hagnesia generator and a conventional radial flux generator.

1.3. Scope of the study

The scope of this study is twofold. Firstly, a generator design based on Hagnesia's patented technology for the IEA 15MW Reference Wind Turbine (RWT) [18] is explained. The design is based on an upscaling of small-scale prototypes that Hagnesia is currently testing. The process uses in-house design tools which were purposely developed for this application. To account for the inherent uncertainty associated with the upscaling process, two "reference" designs are proposed, which differ in both weight and efficiency. As explained in the following, these designs are close to each end of the design spectrum for this size of generator and allow to preliminarily evaluate the importance of parameters such as generator inertia, mass and efficiency on the wind turbine dynamics. The detailed design process and its outcomes are explained in Section 2.

In the second part of the study, detailed load analyses on the IEA 15MW RWT are performed. As detailed in Section 3, in such analyses the reference radial-flux gearless generator is compared to the axial-flux designs by Hagnesia, in order to evaluate the impact of weight on system dynamics. In a following step, constrained tower optimizations are also performed, with the objective of evaluating whether structural mass can be reduced through the use of a lighter generator.

Finally, the most relevant conclusions and impact of this work are summarized in Section 4.

2. Generator design

2.1. Method

The overall workflow for developing a Hagnesia generator design for the IEA 15 MW Reference Wind Turbine (RWT) involves the following key activities:

- Developing and using generator design and assessment tools to explore various design options to define a relevant generator design space based on input requirements, design variables, and optimization targets.
- Conducting in-depth analyses of selected designs to validate both technical feasibility and performance characteristics.
- Generating key design parameters and performance indicators for selected concepts, enabling evaluation of design alternatives from both generator and turbine perspectives.
- To tune and improve design methodologies used based on results and insights from turbine impact studies.

An internally developed design tool—referred to as the Sizing Tool—was employed to generate and evaluate a range of generator design alternatives. Implemented in GNU Octave and Python, the tool enables parameter sweeps across broad design spaces, calculating key design parameters and performance metrics. To ensure credibility, the tool's electromagnetic and fluid dynamic calculations have been validated against detailed 2D/3D FEA and CFD simulations. By combining fixed inputs (e.g., rated power and rated speed) with configurable ranges for selected design variables, the Sizing Tool generates design candidates optimized for objectives such as conversion efficiency or total weight. It outputs detailed results including generator dimensions, performance characteristics (e.g., conversion losses at rated and partial loads), and material usage categorized by type. As part of the FLOATFARM project, new functionality was added to allow input of wind distribution parameters and turbine control settings for torque-speed control. This enables the *Sizing Tool* to optimize generator designs based on annual energy production, taking into account partial-load efficiency rather than relying solely on performance at rated speed. Additional updates include the calculation of generator inertia, which serves as an input for turbine impact studies (see Section 3).With these enhancements, the *Sizing Tool* was used to map feasible generator design spaces and to deliver both key design parameters (for further design studies) and associated performance and material usage data.

Using key design parameters from the Sizing Tool for a selected design, a more detailed mechanical model of the generator was developed in the CAD software Onshape. Table 1 Finite Element Analysis (FEA) simulations, both 2D and 3D, were conducted in Ansys to evaluate and validate the generator's performance across electromagnetic, mechanical, and thermal domains. Modeling the dynamic behavior of the generator presents significant challenges, due to the need for a multi-physics approach that accounts for time- and space-dependent forces acting within and between the generator discs. While this is very computationally demanding, and thus time consuming, the modular and scalable nature of the generator topology enabled the development of a methodology for rescaling FEA-validated designs to a range of possible configurations. As each stator disc is constructed using a set of three-phase segments, as seen in Figure 5, simulation results from a single

three-phase segment can be extrapolated to different generator configurations. This is further described in Section 2.2.1. After evaluating several three-phase segment design options, the decision was made to proceed with the same segment design currently used in ongoing generator prototype projects. While alternative designs may offer better tuned performance—allowing for somewhat lower weight and higher efficiency—this choice provides valuable insight into the scalability and manufacturability of the generator concept, making it more relevant. Figure 5 shows a schematic of the modularity, with few of the possible size configurations.

Based on the FEA-validated three-phase segment, a scaling tool was developed to calculate design and performance characteristics for all possible configurations using this phase segment design. These configurations are defined by the number of discs and the number of three-phase segments per disc, which together determine the machine's diameter and capacity. These were used to assess a relevant design space and produce corresponding design and performance characteristics for possible design configuration, such as size, weight, material use and efficiency (both at rated speed and as a function of torque and speed).

A design configuration with an outer diameter of 8 m, as further detailed in Table 1, was chosen to asses drivetrain integration. It should be noted that this modelling approach is developed to accurately model generator performance and active material use—including NdFeB magnets, copper windings, and electrical steel—while the structural material use relies on less accurate methods. The model used is detailed in Section 2.2.1. A more accurate estimation of the structural material use would require a more relevant model of drivetrain integration and the design loads acting on the generator.

Due to these significant uncertainties in estimating structural mass —which constitutes more than half of the total generator weight— the overall mass predictions should be interpreted with a broad tolerance range of approximately +50% / -25%. Nevertheless, these uncertainties are considered acceptable given the substantial weight reduction compared to the reference generator, especially when factoring in the additional, unaccounted-for mass savings likely achievable in the rest of the nacelle. To evaluate the impact of this uncertainty on overall turbine performance, two generator mass scenarios were considered: a "heavy" configuration, approximately 50% above the estimated mass, and a "light" configuration, roughly 25% below it. This approach also serves to evaluate the trade-offs between generator weight and efficiency, where adding more active material can enhance performance at the cost of increased mass.

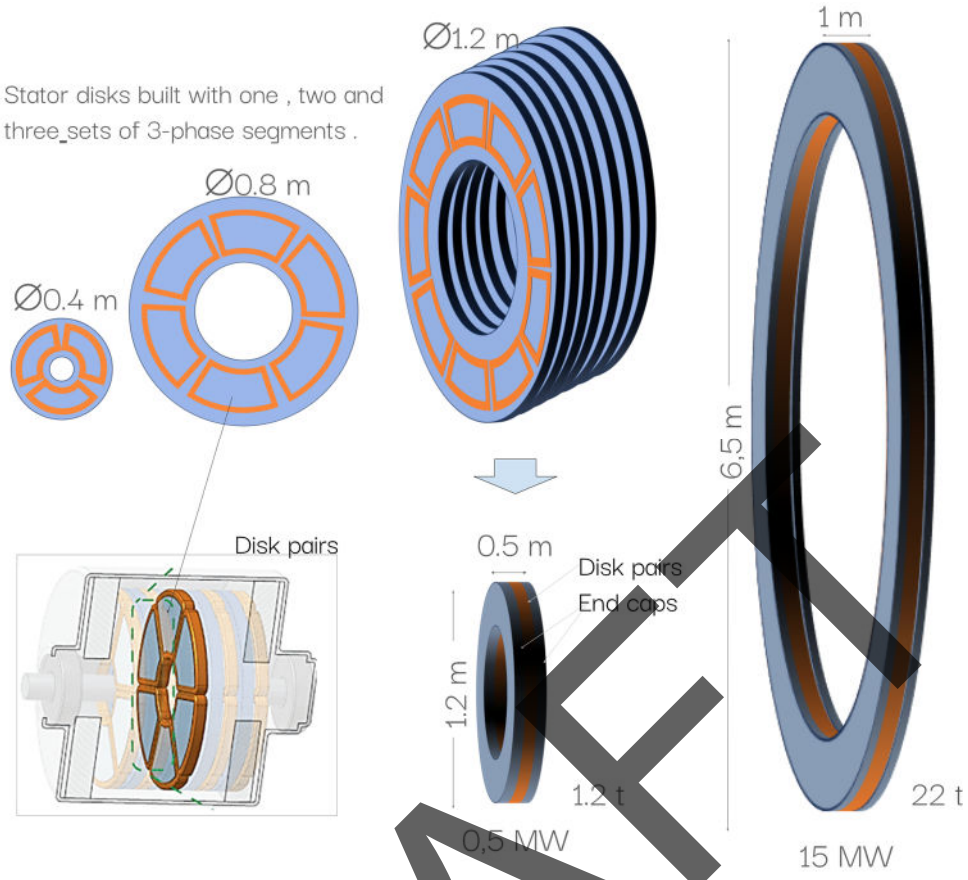

Figure 5 Conceptual illustration of generator modularity and scaling principle, where a generator is built with a certain number of disk pairs (one stator disk + one rotor disk) and each stator disk has a certain set of 3-phase segments. Showing example configurations for the three-phase design chosen for design studies.

FEA modelling and scaling generator characteristics and performance

To evaluate and validate the generator's electromagnetic, mechanical, and thermal performance, finite element simulations were conducted in Ansys using both 2D and 3D models. The electromagnetic analysis was based on the smallest symmetry unit of the machine—a single three-phase segment, illustrated in Figure 5—which was fully modelled in Maxwell. 3D simulations were limited to this individual segment and used axial symmetry to reduce computational effort. Initially, a simplified coil model assuming ideal windings was applied to reduce simulation time, followed by a refined 3D model of one phase, simulated under a limited set of operating points to capture eddy current and proximity effects.

2D simulations were used to enable extensive parameter sweeps and performance mapping at lower computational cost. These models neglect end-effects and therefore tend to overestimate both torque and eddy current losses in the magnets. Correction factors derived from the 3D simulations were applied to improve accuracy. By combining detailed 3D simulations when necessary with 2D sweeps, this hybrid approach enables accurate and scalable electromagnetic modelling of large machines without requiring full geometry modelling.

For estimating fluid losses in-between the disks, a similar approach is used. An Ansys Fluent model of a single rotor-stator disk pair is used for the FEM analysis, calculating viscous losses at different

rotational speeds. These results are then used in the postprocessor to scale the losses according to the number of segments and disks in the given machine configuration.

The validated 3D segment model forms the basis for a scalable methodology, where the full generator is constructed by replicating this unit circumferentially (to increase diameter and torque) and axially (to increase power). Adding more discs scales torque linearly, while increasing the number of segments per disc expands the airgap area and moves the active region outward, resulting in higher torque due to an increased radius. This approach is both physically valid and conservative: as segments are placed further from the center in larger machines, their curvature decreases, simplifying manufacturing and enabling improved copper fill or magnetic loading. These secondary benefits are not captured in the current model, meaning the predicted performance is likely to be underestimated by a small amount.

This methodology ensures that all electromagnetic properties and active material masses—including copper, magnets, and electrical steel—are directly derived from FEM simulations.

The structural material use is modelled as an add-on factor to the active material use, separated per material and also into a rotating and non-rotating part. The add-on factors are based on CAD models from prior design studies and prototype constructions, all of which have so far been conducted on significantly smaller machines. In FLOATFARM, a CAD model was made of the drivetrain integration of the 15 MW Hagnesia generator into the IEA reference turbine, targeting a drop-in replacement without changing any of the other drivetrain components. A simple structural integrity assessment was performed using FEA, applying a static torque load. The analysis aimed to provide an initial evaluation of stress distribution and deformation to ensure a sufficient (over-dimensioned) structural design. By comparing these results with similar design studies for a 2 MW design, the structural material add-on factors were tuned.

2.2. Results

15 MW design options

Based on a parametric evaluation of a wide range of potential generator designs using the Sizing Tool, combined with detailed FEA studies of a few selected three-phase segment designs, one specific phase segment design was selected for further consideration. The FEA-validated results from this design were subsequently rescaled and applied to explore various possible design configurations. Figure 6 presents some key characteristics of the possible 15 MW generator design configurations, shown as a function of the generator's outer active diameter (which corresponds to the number of segments used per disk). Note that an additional 0.2 m should be added to obtain the total outer diameter. Increasing the diameter will increase the airgap speed and also expand the active area per disk, which reduces the number of disks needed to achieve the required power. This, in turn, influences material usage, total weight, and efficiency—as shown in Figure 6. For material usage, the quantities of critical raw materials such as copper and NdFeB magnets are highlighted. In addition, electrical steel is used as an active material, while structural components primarily consist of structural steel, aluminum, and stainless steel.

The efficiency values shown correspond to operation at rated speed and include both electrical losses (resistive losses in the copper windings and frequency-dependent iron losses) and mechanical losses due to viscous drag in the fluid bearings between stator and rotor disks. Since both airgap speed and disc count depend on the generator diameter, these factors will affect overall efficiency. Losses and efficiency can also be calculated across the full range of operational speeds and torques, enabling optimization of annual energy production (AEP) rather than focusing solely on rated-point efficiency. An example efficiency map is shown in Figure 6, based on the design with a 6.7 m outer active diameter.

This 6.7 m configuration is of particular interest as it represents the smallest possible diameter that remains compatible with the main bearing specifications of the IEA 15 MW Reference Turbine. However, for the CAD model shown in Figure 7, an 8 m outer diameter was selected to support a more conservative estimate of structural material requirements for drivetrain integration.

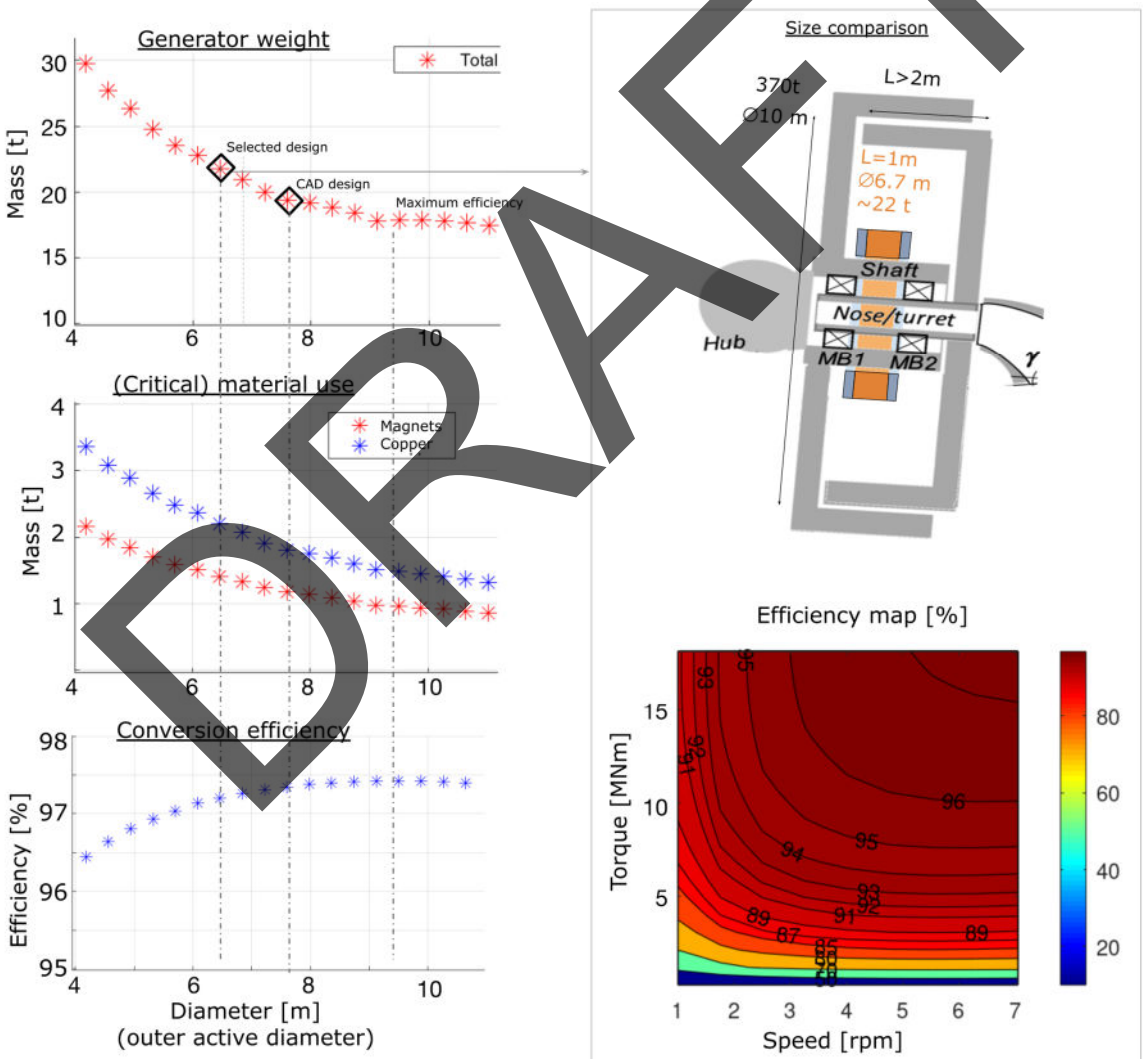

Figure 6 Possible design configurations for a 15 MW direct drive generator, based on a specific phase segment design.

The IEA 15 MW reference turbine with a Hagnesia generator

Figure 7 illustrates the size and shape of the Hagnesia generator in relation to the IEA 15 MW Reference Turbine. The Hagnesia generator is modeled with an outer diameter of 8 m, compared to approximately 10.5 m for the generator in the IEA 15 MW Reference Turbine. The Hagnesia design is also significantly shorter, with a length of 0,75 m versus 2.3 m for the reference generator. The generator could also have been designed with a 6.7 m outer diameter, which would be the minimum diameter to still fit with the bearings used. Such a machine would have a length of 1 m, as further detailed in Table 1.

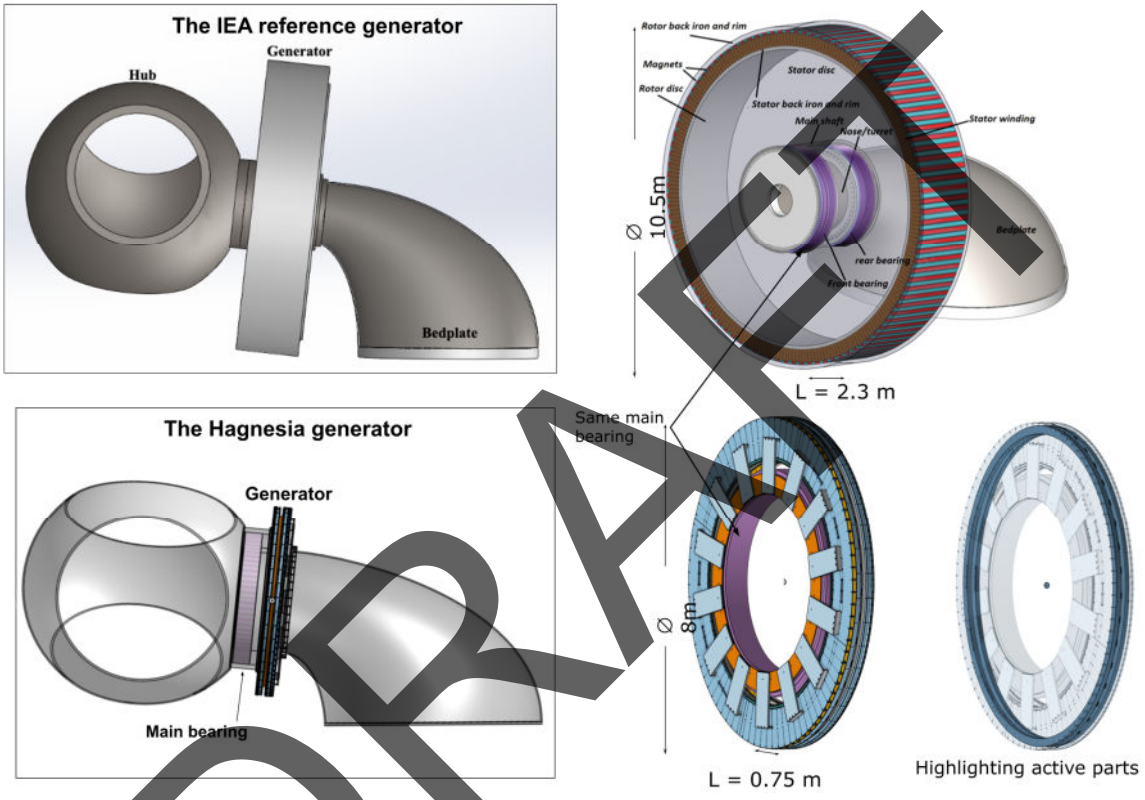

Figure 7 Comparison of generator size relative to the hub, bedplate and bearings of the IEA 15 MW ref turbine.

Table 1 Comparison of weight and material use for some Hagnesia generator configurations, benchmarked with IEA 15 MW ref turbine. Selected cases also marked out in Figure 6.

	IEA 15 MW ref	Hagnesia ø6,7 m	Hagnesia ø8 m	Hagnesia ø9.8 m	Difference	Units
Diameter	10.5	6.7	8	9.8	7-36 %	m
Length	2.3	1	0.75	0.6	57-74 %	m
Total weight	372	22	19	18	94-95 %	t
Magnet	24,2	1.5	1.2	1	94-96 %	t
Copper	9.0	2.2	1.8	1.5	76-83 %	t
Efficiency	96.55	97.3	97.4	97.5	0.8-1 %	%

Table 1 compares a few key characteristics for the generator configurations highlighted in Figure 1, comparing them with the reference turbine. It should be noted that these numbers represent a selection of possible design configurations, based on a specific three-phase segment design. Complementary studies were made with a different phase segment design, which was better tuned to fit a multi-MW design. This resulted in somewhat heavier machines with higher efficiency.

Outlook on turbine upscaling

Using the same phase segment design and scaling methodology, a performance outlook was conducted across a wider range of turbine power ratings. Figure 8 presents the estimated generator weight for the Hagnesia generator (black line), plotted alongside benchmark data for state-of-the-art and promising novel generator technologies — same as those previously shown in Figure 1. This includes results from the GeneratorSE drivetrain optimization model developed by NREL for generators up to 10 MW (red line) [4], as well as extrapolated data for 15–22 MW generators based on conventional radial flux machines (blue line) and a conceptual superconducting generator (orange line) [19]. Both of these larger-scale designs aim to reduce reliance on rare-earth materials. Although the superconducting generator is not yet commercialized, it is projected to achieve up to a 40% reduction in generator weight compared to conventional direct-drive technologies. For additional reference, data points for the IEA reference turbines at 15 MW[18] and 22 MW[20] has been added.

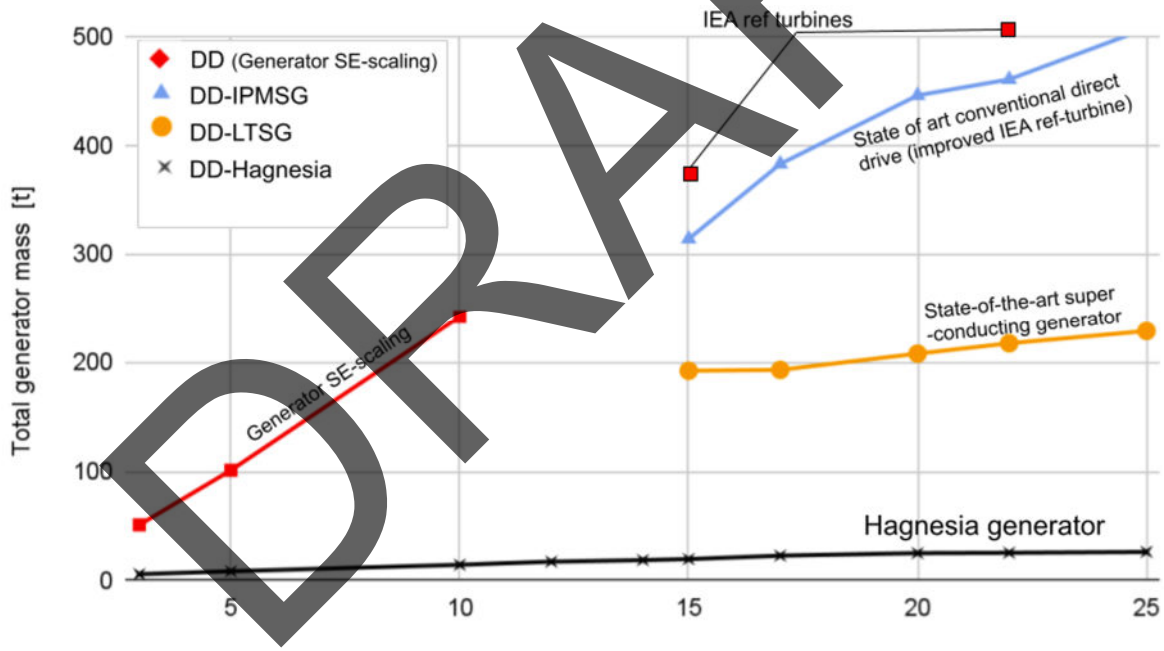

Figure 8 Weight comparison of the Hagnesia direct drive generator to other state-of-the-art generator technologies, as further described in text.

2.3. Discussion and conclusions

The configurations presented represent only a subset of the full design space, constrained to a specific three-phase segment architecture. Adjusting the phase segment design would allow for targeted tuning of key parameters such as weight, material consumption, and efficiency. Nonetheless, the presented information provides a valuable overview of general trends and highlights the trade-offs between size, weight, material use, and performance.

Each of these characteristics has both direct and indirect implications at the generator and turbine system levels, with technological, economic, and environmental consequences that must be evaluated from a holistic, system-level perspective. Material usage is particularly critical, as it strongly influences CAPEX, environmental impact, and supply chain vulnerability—especially given the dependence on critical raw materials. The turbine impact studies presented in this report are an important step in this direction, highlighting the influence of generator mass on FOWT dynamics.

As previously discussed, the generator weight estimates carry a degree of uncertainty, as a complete structural assessment would require a more detailed drivetrain integration study, which is beyond the current scope. Nevertheless, Figure 8 clearly illustrates the strong competitiveness of the Hagnesia concept in terms of material efficiency, further enhanced by its higher electrical conversion efficiency. The potential indirect material saving in other nacelle components – which will be neglected in this study – add an even bigger uncertainty to the nacelle mass estimates

To better evaluate the system-level implications of different generator design configurations—and to account for uncertainty through the use of weight estimation margins—two generator configurations were selected for further turbine-level impact analyses, as detailed in Table 5. The lessons learned from this provide important feedback to the design and optimization objectives used in generator design.

3. Impact on turbine design

3.1. Introduction

In addition to allowing for a significantly lighter gearless generator, with significant weight savings of both structural and active materials, as demonstrated in the previous sections, incorporating this technology may also allow for further weight savings in the tower and substructure. In fact, as discussed in Section 1, inertial and gravitational loads caused by a heavy nacelle, which acts like an inverted pendulum on the tower and substructure, can be significant for FOWTs. The impact of generator weight saving is investigated in this section, using a utility-scale machine with a rated power of 15MW as test-case.

3.2. IEA-15MW RWT

The objective of this preliminary phase of Task 1.2 is to evaluate possible load and mass reductions through the design of a utility-scale machine with a target power of 15MW. The IEA-15MW reference wind turbine on the UMaine VolturnUS-S semisubmersible platform [21] is used as the starting point for all the analysis. At first, in this reference machine the direct-drive generator will be replaced with the Hagnesia concept for a first-step evaluation of possible loads alleviation. The entire Floating Offshore Wind Turbine (FOWT) baseline model of the IEA-15MW RWT is described in WindIO [22] format, which is a parameterized geometry input file for the turbine. The geometry file in WindIO format is required for analysis within the WEIS framework, as it is one of the three necessary input files. The version referenced in this work is v1.1.14, available in the GitHub repository [23] and some of the main structural parameters of the turbine plus semisubmersible VolturnUS-S platform are presented in Table 2.

Table 2 IEA-15MW RWT and VolturnUS-S main structural parameters.

Rated power	15 MW	Rotor position	Upwind	Pontoon width	12.5 m
Rated rotor speed	7.56 RPM	Tower mass	1468 t	Draft	15 m
Hub height	150 m	Generator mass	370 t	Platform radius	70 m
Number of blades	3	Freeboard	15 m	Gen. Efficiency	96.55 %
Drivetrain	direct drive	Columns diameter	12.5 m		
Rotor diameter	240 m	Pontoon height	7.5 m		

The IEA-15MW model presented in version v1.1.14 (referred to as the 'basic model' hereafter) in the GitHub repository was found to have issues concerning the outcoming dynamics of the proposed model, which were found to be significantly different from what is presented in [21] and summarized in Table 3.

Table 3 Rigid Body natural frequencies obtained with QBlade free-decay tests. Values in the *Report* column correspond to the original data provided for the IEA-15MW semisubmersible **[21]**. *Basic Model* column shows the results obtained from free-decay simulations of the GitHub v1.1.14 baseline model, while *Tuned model* column represents free-decay results of the tuned GitHub baseline model.

DOFs	Report	Basic model	Tuned model	Units
Surge	0.007	0.018	0.0078	Hz
Sway	0.007	0.018	0.0082	Hz
Heave	0.049	0.050	0.050	Hz
Roll	0.036	0.038	0.034	Hz
Pitch	0.036	0.038	0.036	Hz
Yaw	0.011	0.0185	0.010	Hz

Free-decay simulations were conducted in QBlade software [24] for the basic model of the IEA-15MW, and the results are presented in Table 3. As observed from the results, the natural periods of the modes—particularly surge, sway, and yaw—differ significantly from those proposed in the report for the basic IEA-15MW model. The discrepancies observed in the natural periods of motion suggest that the mooring lines may possess differing structural properties. As a matter of fact, the structural properties of the mooring lines in the IEA-15MW definition in the GitHub repository differ significantly from those proposed in the Volturn US-S report [25]. To ensure consistency in the dynamic properties of the system, mooring lines structural properties such as extensional stiffness, mass density, drag and added mass were subsequently implemented into the baseline GitHub model of the IEA-15MW. This step was essential, as having a well-tuned geometry input file in WindIO format [26] is crucial for meeting the fixed frequency constraints in the subsequent analysis. The results of the free-decay tests can be found in the 'Tuned Model' column of Table 3. As shown, a well-tuned model was successfully obtained, providing a solid starting point for the following work.

Once the tuning process was completed, it was possible to proceed with replacing the generator using the WEIS framework [1] as described in the following sections. In the analysis, we aim to

evaluate the potential to mitigate loads at the tower base or within the substructure for the Hagnesia generator concepts which are replaced in the tuned design of the IEA-15MW RWT.

3.3. Methods

Before diving into the analysis, a comprehensive overview of the utilized methos is given. The load evaluation and tower optimization leverage a custom coupling between the multi-disciplinary design and optimization framework WEIS and the aero-servo-hydro-elastic time domain simulator QBlade. These two pieces of software have been interfaced within WP7 of the FLOATFARM project to enable multi-fidelity co-design [2]. Figure 9 shows how the main NREL tools are linked in WEIS. WEIS employs the OpenMDAO framework [27], an open-source toolset for formulating and solving MDAO (Multidisciplinary Design Analysis and Optimization) problems. This framework allows for various specific tools, which are needed to compute specific quantities of interest on the various parts of the turbine to be interfaced and thus used in automatic design loops. The toolchain facilitates the optimization of wind turbine geometry and operational parameters, ensuring coherence with design constraints while minimizing an objective function [28]. Examples of the application of WEIS to wind turbine design problems can be found in [29], where more details regarding the structure of the WEIS framework and the recursive connection between the various tools within WEIS itself is also discussed.

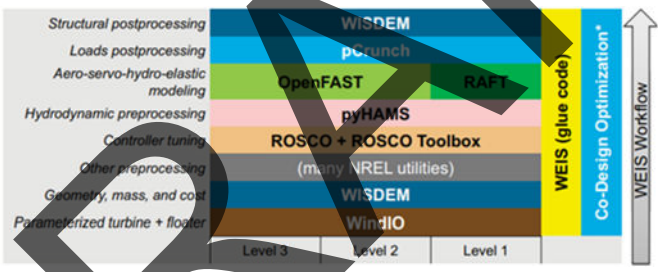

Figure 9 WEIS software stack [1]. WEIS serves as the framework that connects the various analysis and design tools within the workflow. Wind turbine geometry is defined using the WindIO file structure and subsequently converted into a WISDEM model. The controller is managed by ROSCO, while additional utilities developed by NREL facilitate the conversion of the WISDEM system engineering model into higher-fidelity model input files, such as those required by OpenFAST or RAFT. Simulation results are post-processed using WISDEM and pCrunch.

Later in this work, a gradient-free optimization technique is used through the LN-COBYLA optimization algorithm derived from the original COBYLA implementation [30]. While other solvers may be better suited it in specific cases, LN-COBYLA provides more consistent convergence across diverse optimization problems and handles noisy gradients reliably. LN-COBYLA is preferred due to its gradient-free algorithm, which is well-suited for problems that are affected by uncertainty, where numerical convergence towards the global optimum is hard to evaluate due to the noise introduced by uncertainty. Time-domain simulations of wind turbines with turbulent wind and stochastic waves fall within this category and are better suited to gradient-free algorithms such as LN-COBYLA and the NLopt implementation differs from the COBYLA implementation in few ways, including the termination criteria which is incorporated from the NLopt.

3.3.1. Modeling tools

Within the WEIS framework, multiple levels of modeling fidelity can be selected. Optimization can be performed using WISDEM (fidelity level 0), RAFT (fidelity level 1), linearized OpenFAST [31] (fidelity level 2), or OpenFAST/QBlade as higher-fidelity time-domain options. In this study, tower optimizations were run using RAFT, which is a frequency-domain dynamic model that incorporates mooring reactions, hydrodynamics (both strip theory and potential flow), blade element momentum aerodynamics and linear turbine control [32]. RAFT can compute hydrostatic properties as well as system eigenfrequencies. In this study, the minimum frequency to evaluate is set to 0.002 Hz and the maximum frequency is set to 0.6 Hz. The frequency domain representation of the Floating Offshore Wind Turbine system in RAFT results in faster computation and reduced computational cost compared to higher fidelity time domain analysis. In the optimization process, system hydrodynamics are modeled with strip theory (Morison equation) using a drag coefficient of 0.8 and an added mass coefficient of 1.0. Verification of the soundness of this approach is provided in Section 3.2.

In the second part of this work, a load evaluation has been performed. For this aim, QBlade, coupled with WEIS [33], was utilized. Through the coupling, WEIS generates QBlade inputs for the structure, wind and wave field. In this higher fidelity analysis, hydrodynamics are modeled with potential flow elements and the frequency-dependent hydrodynamic coefficients required for the potential flow solution are supplied by a frequency-domain panel code (WAMIT [34]). The hydrodynamic coefficients are functions of body shape, frequency of oscillation and forward speed of the floating body in x-direction [35]. Since the floating platform design is the VolturnUS-S semisubmersible defined by the University of Maine [21] and is assumed to be fixed throughout the optimization process, the hydrodynamic coefficients, as well as the hydrostatic input file which accounts for the restoring provided by the buoyancy, required for the potential flow solution were taken from version v1.1.14 of the IEA-15MW semisubmersible model, available in the GitHub repository [23] and remain unchanged in the analysis.

3.3.2. Environmental conditions

Currently, no standardized design classes have been established specifically for Floating Offshore Wind Turbines (FOWTs), in contrast to their onshore counterparts. Therefore, FOWT designs must be verified under site-specific environmental conditions, considering wind-wave impact loads, hydrostatic forces, and mooring system loads, all of which are influenced by local metocean conditions. In this study, metocean data representative of an offshore location west of the isle of Barra, Scotland, were used to define the sea states under both normal and extreme operating scenarios. The met-ocean conditions are derived from the H2020 project FLOATECH [36].

Table 4 The design load case (DLC) specifications used for design optimization in this study are summarized as follows. For each DLC, every other integer wind speed from 5 to 25 m/s is considered. Wind and wave conditions include the Normal Turbulence Model (NTM), Normal Sea State (NSS), and Severe Sea State (SSS), as defined by IEC standards. The number of wind seeds was selected to ensure a sufficiently comprehensive load set while avoiding excessive computational cost.

DLC	Wind conditions	Wave conditions	Wind seeds	Loads
1.1	NTM	NSS	6	U
1.6	NTM	SSS	6	U

To simulate potentially critical external conditions with various wind turbine operational modes and other design situations and to evaluate the structural response and loading conditions, we referred to Design Load Cases (DLCs) 1.1 and 1.6, defined by the IEC 61400-3 standard [37]. Both DLCs represent normal power production scenarios and utilize a normal turbulence model for the wind field. Specifically, DLC1.1 is primarily used for assessing ultimate loads on the wind turbine structure and components, and a Normal Sea State (NSS) is assumed, where normal wave and wind conditions are expected during standard operation. DLC 1.6 is also designated for assessing ultimate loads but considers a Severe Sea State (SSS) for wave conditions. The significant wave height is determined by extrapolating site-specific metocean data, such that the combination of the significant wave height and the mean wind speed has a return period of 50 years [38]. In all simulations, the wind and wave directions are assumed to be aligned (zero wind–wave misalignment), and the incident wave direction is aligned with the symmetry axis of the floating platform.

For each analyzed DLC we used wind speeds in a range from cut-in speed (3 m/s) to cut-off speed (25 m/s) in 2 m/s increments. Since the optimization analysis was performed using a frequency-domain code, frequencies ranging from 0.002 Hz to 0.6 Hz, with increments of 0.005 Hz, were chosen. These environmental conditions are used not only for the loads analysis process, but also for all the performed optimizations.

3.3.3. Loads analysis

For further evaluating possible loads alleviation by replacing the baseline generator is the first step in this analysis. Two new models are defined by simply replacing the Hagnesia generators into the baseline model of the IEA-15MW turbine. In this preliminary phase of the analysis, only lumped parameters were used to define the generator geometry, including generator mass, moment of inertia, diameter, and electrical efficiency (Table 5). All other nacelle components are assumed to be unchanged.

Table 5 Hagnesia generator design properties

Properties	Units	Lighter	Heavier
Power	[MW]	15	15
Torque	[MNm]	18.9	18.9
Diameter	[m]	10	8.5
Length	[m]	0.6	0.8
Efficiency	[%]	97.5	98.1
Mass	[t]	15	30

A loads evaluation analysis of the IEA-15MW baseline model with the Hagnesia generators is performed using time-dependent simulations in QBlade. For all analyzed designs, the same mean statistical properties of the wind and wave fields are applied, as detailed in Table 4. At each wind speed, six different turbulent wind seeds are used to enable a more detailed and comprehensive load assessment. This approach ensures that the observed load alleviation is consistent across a larger set of operating conditions. Currently, the existing standards do not specify the required simulation

time length for floating offshore wind turbines. For bottom-fixed offshore wind turbine in operating conditions and normal power production (DLC1.1 and DLC1.6), the IEC 61400-3 standard recommends 10-minutes simulations with at least 6-seed for each simulated wind speed, for a total simulation-time of 60 minutes [38]. However, as shown in [39], the semi-submersible platform's dynamic characteristics, particularly its slow natural periods, necessitates the consideration of longer simulation times for accurate fatigue assessment. As a matter of fact, while 10-minute simulations are recommended for many DLCs (60 minutes total stochastic data using 6 seeds), the offshore oil and gas industry uses longer durations (1-6 hours) for floating systems to account for the wave spectral gap, low natural frequencies, and slow-drift effects [38]. For this reason, each simulation is run for 1800 seconds, resulting in a total simulation time of over 10000 seconds for each mean wind speed (30 minutes for each of the 6 seeds). The chosen simulation duration represents a trade-off between the need for longer simulations due to second-order hydrodynamic effects along with the high natural motion periods of the semi-submersible platform and both the realism of the simulated wind field plus computational cost: running turbulent wind simulations much longer than 1 hour may be unphysical and computationally expensive [38]. Time series obtained from the aero-servo-hydro-elastic simulations performed in QBlade coupled with WEIS are then post-processed for load assessment using a python implementation of the open-source code developed by NREL MLife [40].

Aerodynamics in QBlade is modeled using the unsteady BEM formulation for accounting for unsteady phenomena like the atmospheric boundary layer, turbulence and other disturbances. The unsteady BEM formulation makes use of a polar grid for the azimuthal discretization of the inductions factors as explained in [41]. This method allows for the account of azimuthal variation of the induction which changes among blade span due to 3D effects. The wave field in QBlade is modeled using linear wave theory (Airy waves), enabling the generation of both regular and irregular waves. Irregular waves are represented as a superposition of regular wave components [24]. The wave field is defined by specifying several parameters that characterize the wave spectrum, including the significant wave height, spectral peak period, wave direction, spectral type (JONSWAP in this case), and the discretization of the energy spectrum. Discretization involves dividing the spectrum into bins, each containing an equal amount of energy. In this work, a frequency range from 0.001 Hz to 1 Hz is used, and the spectrum is discretized into 18000 bins. Within QBlade, structural dynamics is modelled based on the finite element analysis (FEA) module of the opensource multi-physics simulation engine Project Chrono [42]. In this formulation, the turbine structural model consists of multiple body objects for the blades and the tower, each modeled following the Euler-Bernoulli beam formulation allowing for combined rigid body and deformation analysis. Aerodynamics is then coupled with structural dynamics with a loose coupling approach [43]. As proposed for the baseline model of the IEA-15 MW wind turbine, the ROSCO controller [44] is employed in this study. The ROSCO controller is a modular, open-source wind turbine control framework designed to replicate the operational functions of standard industry controllers. It includes features suitable for both fixed-bottom and floating wind turbines and has a fixed architecture that can be adapted to various turbine models by acting on gains and setpoints. With only a few tuning parameters, the complete controller configuration can be generated using an automated tuning routine [44]. The ROSCO controller is also provided with a floating offshore wind turbine feedback module which helps to stabilize the platform motion by adding damping to the platform itself and avoiding the negative-damping problem [45]. The floating feedback uses inputs coming from rotor motion to stabilize the platform allowing for a decoupling of the generator speed dynamics and platform motion. In this work, the main

controller features are set as for the baseline IEA-15MW RWT as specified in the DISCON file available on the GitHub repository of the turbine [46].

With this simulation set-up, the two modified versions of the IEA-15MW with the Hagnesia generators are compared against the baseline tuned model of the IEA-15MW described in Section 3.2.

IEA-15MW with Hagnesia generators

In this phase the two modified versions of the IEA-15MW were examined. These models consist of the baseline IEA-15MW where the direct-drive generator is replaced with the two designs of the Hagnesia generator: the heavy and the light configuration. Hereafter, the two models are referred to as "IEA Light", representing the IEA-15MW equipped with the lighter Hagnesia generator, and "IEA Heavy", representing the IEA-15MW equipped with the heavier Hagnesia generator. DLC1.6 has been analyzed in order to compare the extreme loads on the turbine during operation. DLC1.6 has been selected as it has shown to be particularly severe for FOWTs, especially in the harsh met-ocean conditions that are considered herein [47]. A summary of the loading statistics on key turbine components shown in Figure 10. In Figure 10, the shaded area indicates the standard deviation, while the dots represent the mean of the maxima (values above the mean) and the mean of the minima (values below the mean) across all seeds for each mean wind speed, estimated as recommended by the standards [48]. Triangles denote the maximum and minimum values recorded for each wind speed. The results show that a reduction in both the mean load values and the mean values of the overall load maxima for each seed can be achieved. This is primarily attributed to the decrease in gravity and inertial loads resulting from the reduced mass at the top of the tower. The load alleviation effect is considerable when designs with reduced Rotor-Nacelle Assembly (RNA) mass, due to lighter a generator, are evaluated. Notably, the fore-aft bending moment in the y-direction (TwrBsMyt) is reduced. The mooring line tension of the line positioned in the upwind direction (Ten ML1 in Figure 10) appears to be only marginally influenced by the generator's weight. In fact, loading on the upwind mooring line is mainly driven by the surge displacement of the platform, which, as shown in Figure 10, is mostly unaffected by the reduction in generator weight. In fact, the surge position of the turbine is primarily influenced by external loads, such as hydrodynamic forces and rotor aerodynamic thrust, which slightly change across the presented simulations.

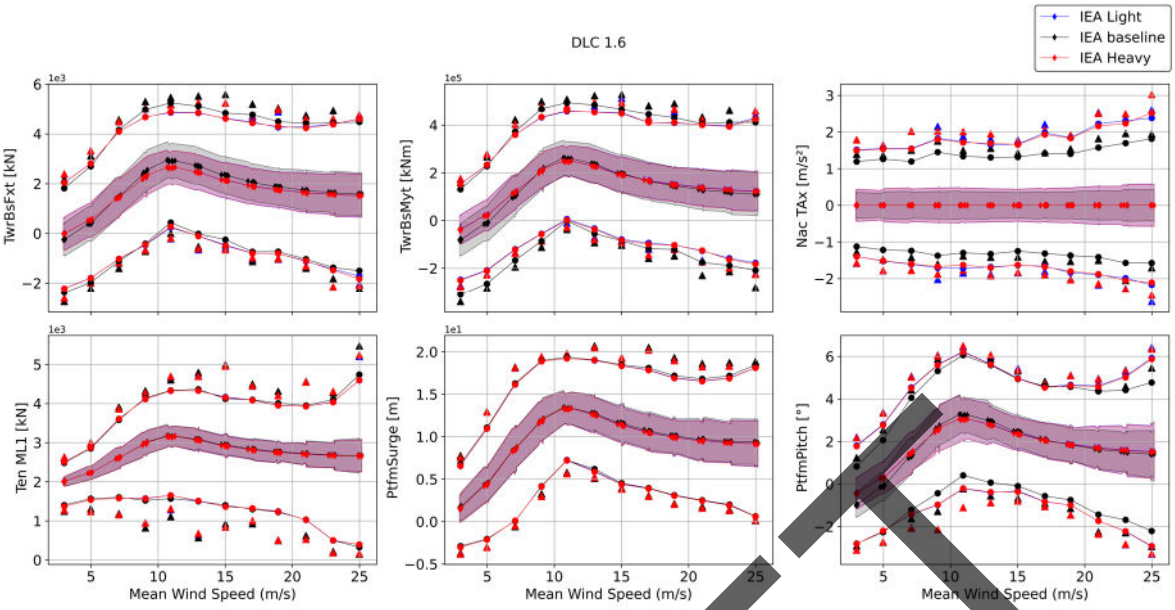

Figure 10 Comparison of tower base force in x direction (TwrBsFxt), tower base bending moment in y direction (TwrBsMyt), nacelle fore-aft acceleration (Nac TAx), upwind mooring line tension (Ten ML1) and platform displacement in x-direction (PtfmSurge) along with platform pitch (PtfmPitch) mean value, standard deviation (shaded), maxima and minima per wind speed recorded in DLC 1.6. Triangles refer to DLC 1.6 maxima and dots are referred to DLC1.6 means of maxima.

The maximum and minimum values of the nacelle acceleration in the out-of-plane direction (Nac TAx in Figure 10) are significantly higher in magnitude compared to the baseline IEA-15MW model, with an outlier for the IEA-15MW with the Hagnesia generator systems (both heavier in red and lighter in blue) is observed at approximately 23 m/s. To provide a more detailed analysis of this behavior, we can refer to Figure 11 where Power Spectral Density (PSD, on the left) and time series (on the right) are reported for the simulation in which the maximum value of nacelle acceleration is recorded. Only a subset of the most relevant load sensors is shown for brevity in the low and wave frequency ranges. Very little energy was found in the signals at higher frequencies. This figure provides a comparison between the three analyzed systems, with all shown quantities corresponding to a wind speed with a mean value of 23 m/s, choosing the seed in which the outlier in nacelle acceleration, observed in Figure 10, occurs. The peak period of the wave (around 18 seconds), clearly shown in the PSD of the wave elevation, is reflected in all the other quantities which are highly influenced by the wave, such as the platform pitch and nacelle acceleration. The time series of nacelle acceleration (Figure 11) clearly shows the outlier value at approximately 700 s, most likely caused by an extreme wave approaching the FOWT. The higher nacelle acceleration may be, at least in part, due to a combination of higher pitch motion and higher tower deflection.

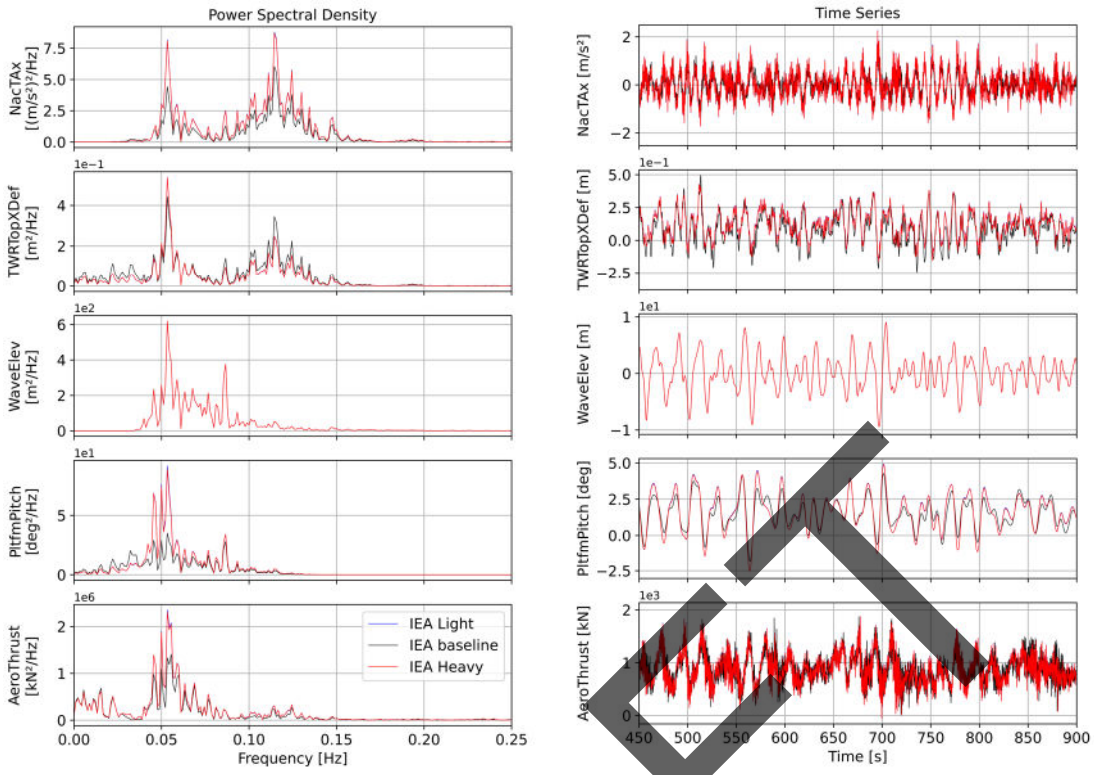

Figure 11 On the left, comparison between the three models (IEA Light, IEA baseline and IEA Heavy) of the Power Spectral Density (PSD) of nacelle fore-aft acceleration (NacTAx), tower top deflection in x direction (TWRTopXDef), wave elevation (WaveElev), platform pitch (PltfmPitch) and aerodynamic thrust (AeroThrust). On the right, the corresponding time series is shown. All the plots refer to a mean wind speed of 23 m/s in DLC1.6.

In the shown frequencies range in Figure 11, nacelle acceleration PSD in fore-aft direction is higher in magnitude in the cases with Hagnesia generator (it can be seen also in Figure 10). More in detail, two distinct peaks in the spectrum can be noted, one from approximately 0.04 Hz to 0.08 Hz, and the other ranging from 0.08 Hz to approximately 0.15 Hz. The increase in nacelle acceleration in the lower peak appears to be correlated to an increase in platform pitch motion at these frequencies. As shown in Table 8, rotational inertia is significantly lower in the systems which use the lighter, Hagnesia-designed, generators. Among others, the pitch motion of the platform is influenced by wave excitation within the frequency range. In the shown cases (IEA Light, IEA Heavy, and the baseline IEA-15MW RWT), the hydrodynamic loads (wave conditions) and platform geometry are the same. The only difference among these systems is the lower rotational inertia of the IEA Light and IEA Heavy configurations compared to the baseline IEA-15MW, which may lead to a higher magnitude in the platform pitch power spectral density. The PSD of platform pitch is slightly higher even in the 0.08-0.15 Hz range for the turbines with the lighter generators, although the amplitudes of the spectra in this region are much smaller. In this frequency range, nacelle acceleration is strongly correlated with tower-top deflection (Figure 11). More in detail, the nacelle acceleration is higher than the tower top displacement in x-direction, indicating faster tower-top motion (higher acceleration) but with smaller amplitude (lower x-displacement), which is again attributed to the lower mass at the tower top.

Figure 12 shows the ratio between the maximum of the main loads mean of maxima (evaluated as recommended in [48]) in the IEA-15MW turbine with Hagnesia generators (both heavy and light

designs) and those recorded for the IEA-15MW baseline tuned model expressed as relative percentage. The figure highlights the reduction in maximum loads achieved by using a lighter generator. Even in the mooring line tension there is a reduction in the maximum load, while, as explained previously, the nacelle acceleration is higher in the systems with Hagnesia generators.

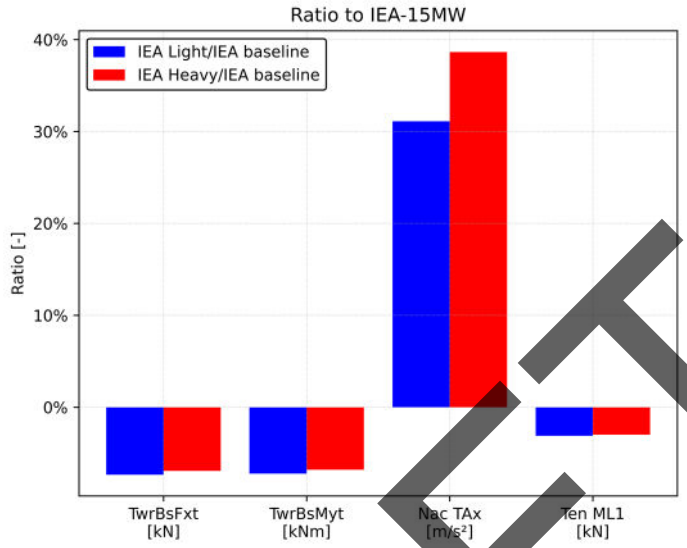

Figure 12 In red, the ratio (expressed as a relative percentage) of the mean extreme load values for the IEA-15MW turbine with the heavy Hagnesia generator to that of the baseline IEA-15MW turbine. In blue, the same ratio for the IEA-15MW turbine with the light Hagnesia generator, relative to the baseline model.

A comprehensive fatigue load assessment requires a large number of simulations under Normal Sea States (NSS), accounting for a wide range of wind speeds, wind–wave misalignments, significant wave heights, and wave peak spectral periods. However, in this study, a preliminary evaluation of fatigue loads is presented, focusing on load analysis under normal operating conditions.

Fatigue loads are estimated in DLC 1.1 and post-processed using the methodology described in [47], using the damage equivalent loads metric. Results are presented in Figure 13. The short term, 1 Hz zero-mean Damage Equivalent Loads (DELs), are useful criteria to quantify fatigue loads: they represent a constant-amplitude fatigue-load that would produce the equivalent amount of fatigue damage as the actual variable load experienced by a system component over a given period [48]. The Palmgren–Miner linear damage accumulation hypothesis is applied to compute the DELs from the time series data obtained from load sensors. These time series are post-processed using a rainflow counting algorithm [49]. DELs are computed as follows without using the Goodman correction [48]:

$$DEL_j^{ST} = \left(\frac{\sum_i \left(n_{ji} \left(L_{ji}^R \right)^m \right)}{n_j^{STeq}} \right)^{\frac{1}{m}}$$

where n_{ji} is the ith cycle count for time-series j, n_j^{STeq} is the total equivalent fatigue counts for time-series j, L_{ji}^R is the load range for cycle i and time-series j and *m* is the Whöler exponent of the inverse S-N curve which is set to 4 for tower and to 10 for blade root fatigue loads [49].

Figure 13 shows a comparison between DELs and standard deviation of some of the main analyzed fatigue loads and it is noticeable that there is a reduction in DELs at the tower base sensors for the

IEA-15MW with the Hagnesia generators. A slight increase in the blade root bending moment is also observed, which may be attributed to the higher nacelle acceleration as reported in Figure 10. Standard deviation box plots on the left of Figure 13 show statistically higher values for the IEA-15MW baseline model meaning that loads have a greater variability with respect to the mean value (higher loads amplitudes).

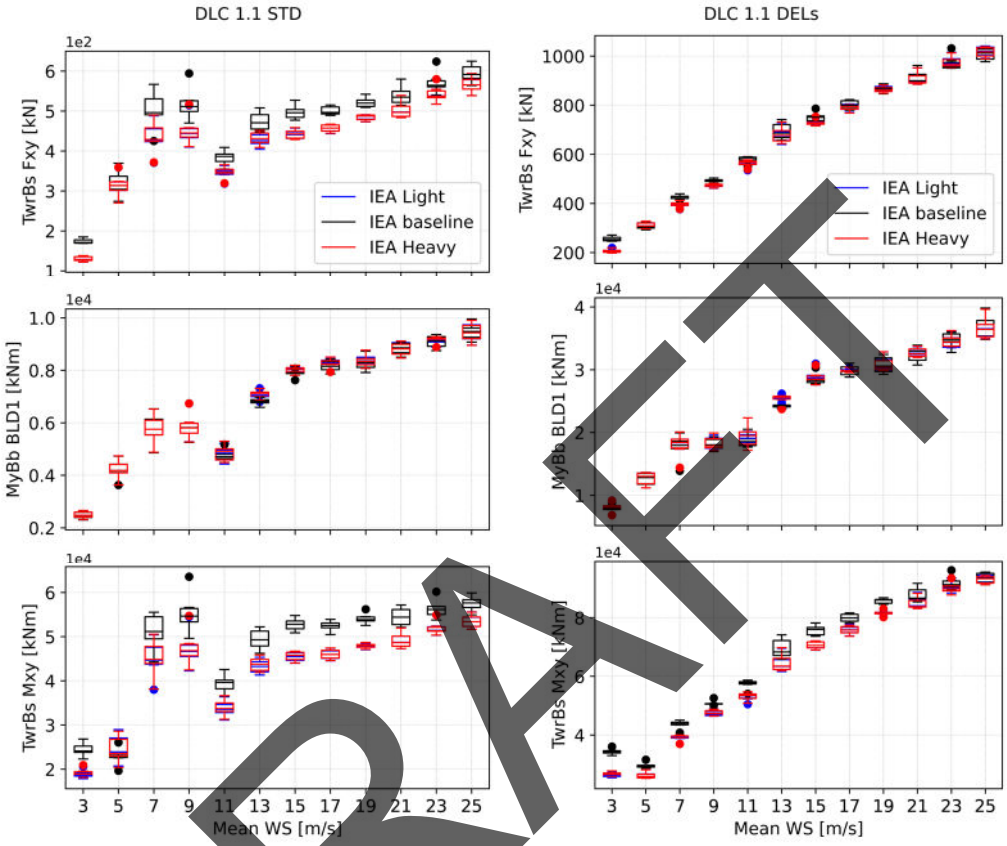

Figure 13 On the left, box plots of the standard deviation of the tower base force in the xy-plane (TwrBs Fxy), blade root bending moment in the y-direction (MyBb BLD1), and tower base bending moment in the xy-plane (TwrBs Mxy) are shown. On the right, 1-Hz zero mean DELs are plotted as a function of mean wind speed. Three cases are compared: the IEA baseline, and the IEA-15MW turbine equipped with lighter blue) and heavier (red) Hagnesia generators. In this plot, the solid line within each box represents the median; boxes indicate the first and third quartiles, and the whiskers represent the 5th and 95th percentiles across the six seeds simulated for each mean wind speed value.

Nevertheless, from this analysis, it is possible to conclude that reducing generator mass reduces fatigue loads. The observed reduction in fatigue loads and extreme loads indicates an overall reduction in tower loading. This, in turn, indicates that material savings in the tower are at hand. This possibility is explored in the following paragraphs.

This analysis demonstrates that load alleviation is achievable through the usage of the Hagnesia generator concept. Consequently, the potential for further load mitigation and reduction in raw material usage is investigated by redesigning the tower of the baseline IEA-15MW Reference Wind Turbine (RWT). The objective is to reduce the tower mass by varying its diameter and wall thickness within an optimization routine conducted using the WEIS framework. A detailed explanation of the optimization problem is provided in the following.

3.4. Optimization problem definition

As mentioned in Section 3.3, the WEIS framework integrates various software tools using OpenMDAO and for all the optimization processes in this work, the COBYLA solver is used due to its derivative-free iterative approach. In this section, a more in-depth explanation of the merit figure, design variables and constraints of the optimization loop is supplied.

The objective of the optimizations that were performed withing this task is the evaluation of the potential structural mass that can be saved by using a lighter direct-drive generator in place of the standard one that is used in the reference design. The generator parameters in the baseline geometry of the tuned IEA-15MW model were modified to incorporate the Hagnesia generators, whose properties are listed in Table 5. Hagnesia provided two alternative generator designs: one with reduced mass at the expense of lower efficiency, and the other featuring higher efficiency but with an increased mass. Nevertheless, both proposed designs exhibit significantly lower mass (over ten times lighter) compared to the 370-ton generator used in the original IEA-15MW baseline model. The IEA 15 MW generator was replaced with a simplified model of the Hagnesia generator in the turbine geometry file. In this preliminary phase of the analysis, only lumped parameters were used to define the generator geometry, including generator mass, moment of inertia, diameter, and electrical efficiency (Table 5). All other nacelle components are assumed to be unchanged. Given the significant reduction in overall Rotor-Nacelle-Assembly (RNA) mass of about 35%, this assumption is clearly conservative, as additional structural mass can likely be seen in the yaw bearing, main shaft and nacelle housing. The merit figure in the optimization analysis is the tower mass. The aim of the optimization is to achieve a lighter tower, as it is required to withstand a reduced peak load compared to that of the original IEA-15MW design as well as fatigue loads as shown in Figure 13. As previously discussed, a comprehensive fatigue load analysis was not conducted in this study, as it would require a significantly wider design space. It must be noted that fatigue load is not a design driver in the optimization process at this stage, since it is not imposed as a constraint.

3.4.1. Design Variables

The design variables selected for this analysis are the tower diameter and the thickness of its structural layers. The tower is modeled with eleven breakpoints, evenly spaced at intervals of approximately 13 meters where every point is defined in terms of outer diameter and wall thickness. This discretization is unchanged from the reference 15 MW design. Both geometrical parameters significantly influence stress distribution and the structure's susceptibility to buckling along its height. Satisfying buckling and stress constraints is a key driver in both the optimization process and the final design. A total of 22 design variables are considered: eleven for the diameter and eleven for the thickness of each breakpoint.

3.4.2. Constraints

In the optimization process, the objective is to maintain the tower's natural frequencies above the blade passing frequency (3P) range. In floating wind turbine systems, tower should be designed such that its fore-aft and side-side natural frequencies are higher than both the rotor's rotational frequency (1P) and the blade passing frequency (3P), resulting in a stiff–stiff tower configuration [19]. This design approach helps to avoid potential resonance issues whereas, a soft–stiff configuration, characterized by lower natural frequencies, would require more sophisticated control strategies to

ensure dynamic stability. The 3P frequency of the IEA-15MW Reference Wind Turbine (RWT) is around 0.38 Hz. Accordingly, one of the constraints imposed in the analysis is that the first natural frequency (f_1) of the coupled floater–tower system must exceed 0.45 Hz. This margin ensures that the first natural frequency of the tower alone, which is expected to be slightly lower, remains safely above the 3P excitation range.

Another constraint is the von Mises stress constraint among tower sections. In the structural analysis, the tower is required to remain within allowable ultimate stress limits for steel. To prevent structural instability under applied loads, both global and shell buckling constraints are enforced following Eurocode guidelines [50]. All these three constraints for steel are evaluated in the WEIS structural post-processing phase, after the loads are calculated along the tower length.

Additional geometric constraints are applied to control the shape of the tower. Slope and taper constraints enforce a continuous reduction in diameter from the base to the top of the tower, with each segment tapering in a physically and practically reasonable way. Similarly, thickness slope constraints are introduced to ensure that the total wall thickness across each tower segment generally decreases from bottom to top. Design variables and constraints are summarized in Table 6.

Table 6 Design Variables and Constraints

Design Variable	Lower bound	Upper bound	Constraints	Lower bound	Upper bound
diameter	6.5 m	10 m	f1	0.45 Hz	0.55 Hz
layer thickness	0.004 m	0.10 m	stress		true
			global buckling		true
			slope		true
			thickness slope		true

3.4.3. Optimization results

With reference to the previously described optimization problem, several analyses were performed. First, the tower was optimized using both generator designs proposed by Hagnesia, and the differences between the resulting systems were analyzed. Subsequently, a load assessment was conducted for a hybrid design, consisting of the IEA-15MW RWT with Hagnesia generators, both the lighter one and the heavier one. Finally, a comprehensive load analysis was performed, comparing the load obtained for the IEA-15MW baseline model with the results obtained from the optimization.

Lighter Hagnesia Generator

To optimize the IEA-15MW RWT tower supplied with the Hagnesia generator, generator's baseline design properties (summarized in the "Lighter" column of Table 5)were replaced into the WindIO geometry file. The optimization process was conducted as previously described, with a maximum of 600 iterations imposed. In Figure 14-a, convergence trend of mass optimization is shown in comparison to baseline IEA-15MW RWT tower mass. Due to the high number of design variables, the tower mass requires many iterations to converge. As mentioned previously, the optimization process is defined by constraints on design variables, merit figure, and user-imposed tolerances. In each iteration, the LN-COBYLA algorithm ensures the integrity of the constraints while minimizing the

merit figure (function $f(x)$) varying design variables. by varying the design variables. Each constraint can be expressed as a function $c(x)$, subject to:

$$c(x) \leq b$$
$$x^{min} \leq x \leq x^{max}$$

where x is the vector of design variables used to calculate the merit figure $f(x)$. The b parameter represents the bound imposed in the inequality constraints, and both x^{min} and x^{max} are the bounds for the design variables. The convergence criteria used by LN-COBYLA requires that the iterations stop when the difference between the current merit figure value ($f(x_i)$) and the previous one ($f(x_{i-1})$) is lower than the user-imposed tolerance:

$$|f(x_{i-1}) - f(x_i)| \leq \varepsilon$$

In this analysis, ε is imposed equal to $1E^{-3}$. However, the iterative convergence process can also end when the maximum number of iterations is reached by the algorithm (set to 600 in this analysis), and this is what occurred, the convergence process ended because of the maximum iteration limit imposed. As shown in Figure 14-b, which presents a comparison between the geometry of the IEA-15MW RWT and that of the newly optimized turbine.

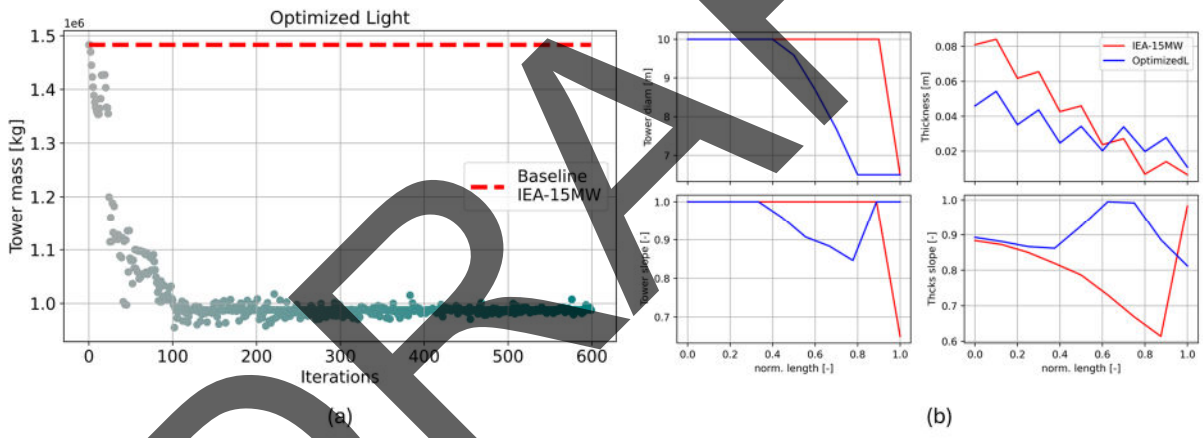

Figure 14 Lighter Hagnesia Generator tower optimization, (a) shows merit figure (tower mass) convergence trend compared with base line IEA tower mass. Comparison between IEA-15MW RWT geometry and optimized tower is shown in (b).

Nevertheless, this does not imply that the routine was unable to reach a satisfactory design point, as the failure to meet the convergence criteria can be seen because of numerical noise (dispersion near 600 iterations in Figure 14 (a)), rather than a failure to converge to an optimal point. In fact, the solver considers the last calculated point (iteration 600) as the optimal one. Due to the presence of numerical noise in the convergence process, the final solution may not be the overall optimal point: for this reason, the tower mass, which is the objective function, may oscillate around the actual optima by a few tons. However, given the significant reduction in tower mass with respect to the reference design that has been achieved, this level of numerical convergence towards the optimal solution was considered sufficient. The system obtained through this optimization will be referred to as 'Optimized Light' hereafter, indicating that it corresponds to the system optimized using the Hagnesia light generator.

Heavier Hagnesia Generator

A separate optimization was performed also using the heavier and more efficient design proposed by Hagnesia. To optimize the IEA-15MW RWT tower with the drop-in replacement Hagnesia generator, the baseline design properties of the generator (summarized in the "Heavier" column of Table 5) were replaced in the WindIO geometry file. The same settings, objective function and constraint as previously described were used in the optimization process, including the maximum of 600 iterations limit. As shown in Figure 15 even this time the imposed number of iterations was not sufficient to achieve convergence, although the solution appears significantly more stable, suggesting that convergence may be near. Given the high number of iterations required to reach a stable solution, the use of the frequency-domain code RAFT is recommended, particularly due to its higher computational speed compared to a time-domain code such as QBlade, which would be much more resource-intensive from a computational perspective. This system will be referred to as 'Optimized Heavy', following the same naming metric used for the 'Optimized Light' system.

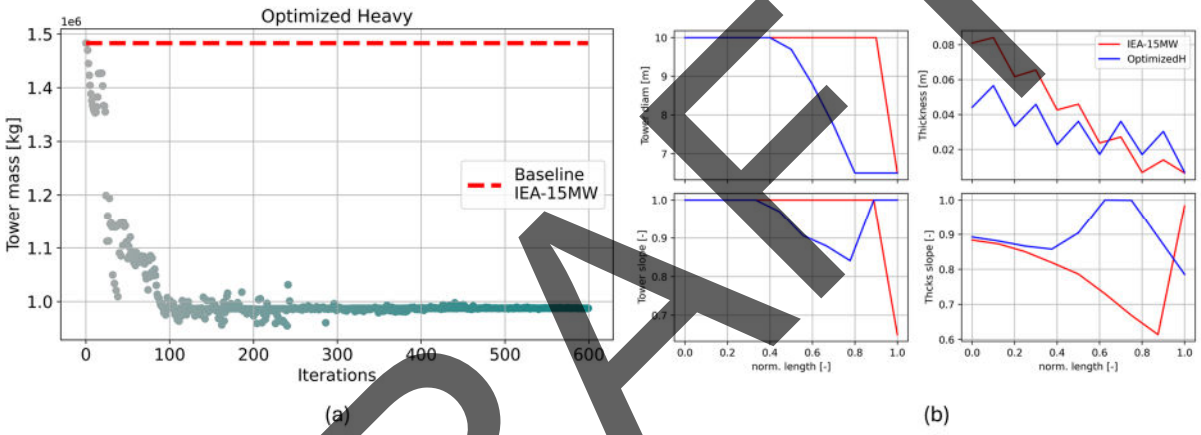

Figure 15 Heavier Hagnesia Generator tower mass optimization, (a) shows merit figure (tower mass) convergence trend compared with base line IEA tower mass. Comparison between IEA-15MW RWT geometry and optimized tower is shown in (b).

In both the lighter and heavier cases, tower mass is significantly lower compared to the baseline tuned model of the IEA-15MW. In fact, thanks to this new generator technology, the tower mass can be reduced by up to 30%. Main structural properties resulting from this optimization such as tower mass, fore-aft frequency (f_1) of both tower and substructure are summarized in Table 7. Nevertheless, although the reduction in tower mass is significant, it is important to note that the tower geometry is strongly influenced by aerodynamic loads, which are the primary drivers in the design of both the tower and the substructure [19]. The two optimized designs have a marginally lower fore-aft frequency in both tower and substructure compared to the IEA-15MW models, as indicated in Table 7. However, the first natural frequency of the substructure lies above the 3P excitation frequency, satisfying the frequency constraints imposed during the optimization and resulting in the required stiff–stiff design for the floating tower.

Table 7 Comparison between structural properties of analyzed geometry

Properties Output	Units	IEA-15MW	Tuned IEA-15MW	Optimized Light	Optimized Heavy
tower mass	[kg]	1483	1401	988	987
tower f1	[Hz]	0.3754	0.3656	0.3436	0.3428
substructure f1	[Hz]	0.5242	0.51	0.4436	0.45
surge	[Hz]	0.007	0.0078	0.0083	0.009
sway	[Hz]	0.007	0.0082	0.009	0.009
pitch	[Hz]	0.036	0.036	0.045	0.044
roll	[Hz]	0.036	0.034	0.044	0.044

In addition to evaluating the global turbine characteristics in Table 7, it is also interesting to discuss the rotor properties, as shown in Table 8. The rotor's moment of inertia is a key factor in determining the behavior of the floating offshore wind turbine (FOWT), as it directly influences the inertial and gravitational loads acting on the tower and substructure, as well as the system's dynamic response and the natural frequency of the turbine–controller system [51]. The rotor's moment of inertia is influenced by the generator's inertia, which contributes to its overall value. For this reason, replacing the generator in the FOWT system could impact its dynamic behavior. Table 8 lists the moment of inertia about each component's axis of rotation. As shown in the table, the generator's inertia is negligible compared to the total rotor inertia, indicating that the generator's geometry has little influence on the overall dynamics. If Hagnesia's generators are integrated into the FOWT system, the generator's inertia accounts for only 0.03% to 0.04% of the total rotor assembly inertia, meaning it has a very limited impact on the system's dynamic behavior. Referring to Table 8, the last row illustrates the marginal influence of the generator mass relative to the total mass of the wind turbine system. Specifically, the percentages presented represent the ratio of the generator mass to the overall system mass. In the baseline configuration, the generator contributes approximately 2% of the total system mass. In contrast, for the systems with the Hagnesia generators, this contribution decreases significantly, ranging from only 0.0779% to 0.1558%. This straightforward comparison highlights that a 15-ton variation in generator mass has a negligible effect on the overall mass of the wind turbine system. Consequently, as shown previously, the two optimized systems utilizing Hagnesia generators exhibit very similar structural and dynamic behavior, with negligible differences in tower properties, as shown in Table 7.

Table 8 Inertia properties of main rotor components, center of gravity (COG) z position of the total wind turbine system and ratio of generator mass to total wind turbine system mass in percentage (gen mass %).

Inertia [kg·m²]	Baseline IEA-15MW	Optimized Light	Optimized Heavy	IEA Light	IEA Heavy
Generator	1.84E+06	9.38E+04	1.35E+05	9.38E+04	1.35E+05
Hub	1.04E+06	1.04E+06	1.04E+06	1.04E+06	1.04E+06
Rotor	2.86E+08	2.86E+08	2.86E+08	2.86E+08	2.86E+08
Total	2.89E+08	2.87E+08	2.87E+08	2.87E+08	2.87E+08
%	0.636	0.0327	0.0472	0.0327	0.0472
zCOG [m]	0.260	-4.397	-4.329	-3.116	-3.034
gen mass %	1.922	0.0779	0.1558	0.0779	0.1558

Loads analysis for the optimized systems

Loads assessment has been conducted for the two wind turbine systems obtained as described in Section 3.3.3. Figure 16 shows an overview of the statistical values for main loads sensors at tower base, tower top and the nacelle acceleration. The plotting metric is the same as explained in Figure 10. Considering Figure 16, it can be observed that loads reduction is even more significant than what is shown in Figure 10. This effect is primarily attributed to the reduced tower mass and diameter, which leads to lower gravitational and inertial loads. On the other hand, nacelle acceleration is increased even with respect to the increases that were noted previously, where the tower was left unchanged with respect to reference design.

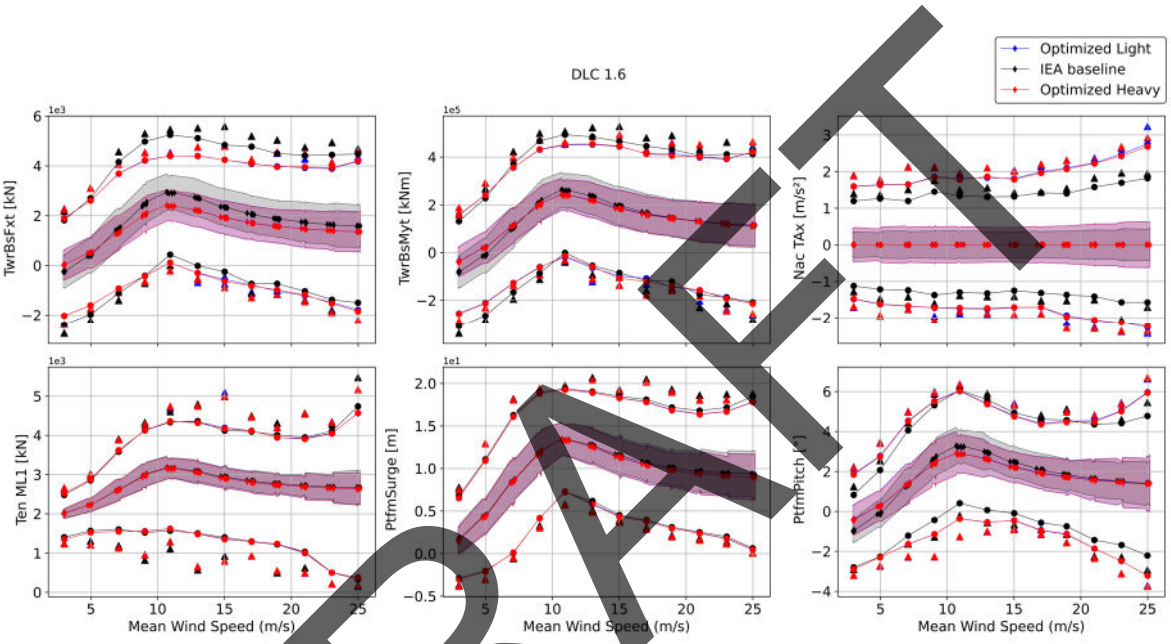

Figure 16 Comparison of tower base force in x-direction (TwrBsFxt), tower base bending moment in y-direction (TwrBsMyt), nacelle fore-aft acceleration (Nac TAx), upwind mooring line tension (Ten ML1) and platform displacement in x-direction (PtfmSurge) along with platform pitch (PtfmPitch) mean value, standard deviation (shaded), maxima and minima per wind speed recorded in DLC 1.6. Triangles refer to DLC 1.6 maxima values and dots are referred to DLC1.6 means of maxima.

From the Power Spectral Density and time series shown in Figure 17 of the most relevant loads sensor is clearly visible how a combination of higher pitch motion of the platform coupled with a higher tower flexibility leads to higher nacelle acceleration. The reasons for the observed behavior are found to be largely the same as discussed previously when comparing the designs with the Hagnesia-proposed generators mounted on the IEA 15MW RWT reference tower to the IEA 15MW RWT with the reference generator. The lower rotational inertia of the designs with lighter tower and generator lead to increased pitch motion, which in turn causes higher inertial loading. In addition, the optimized, lighter, tower designs are more flexible, increasing RNA acceleration and inertial loads even further.

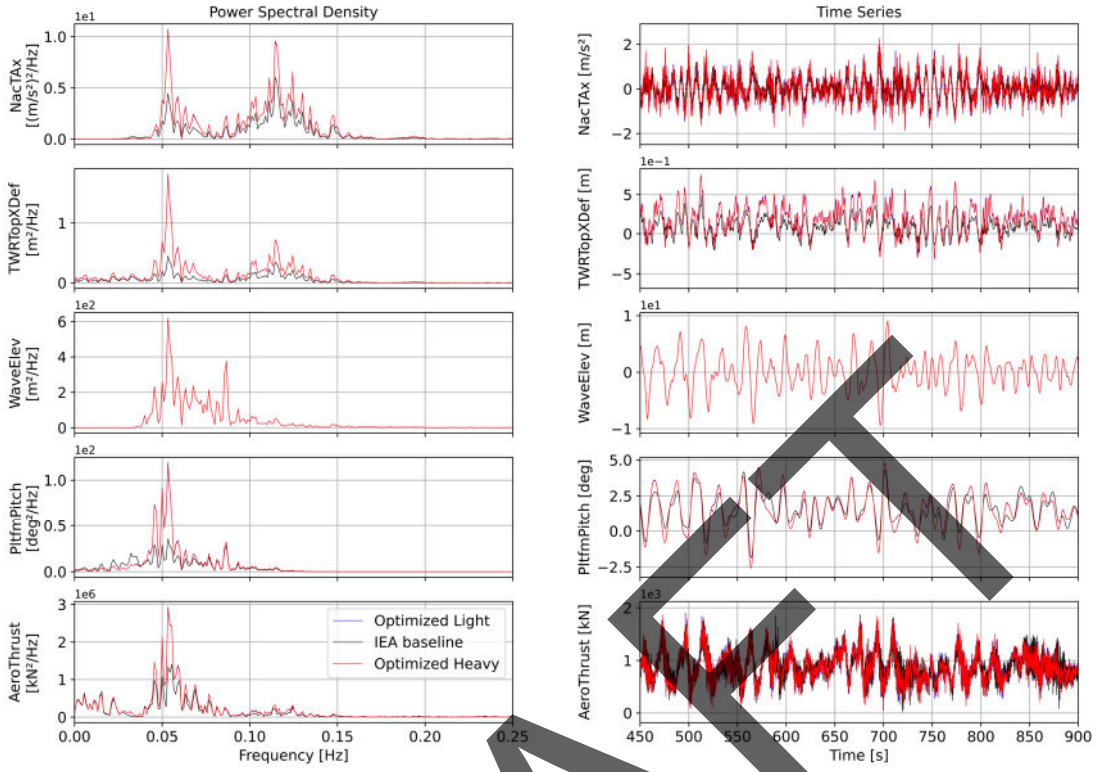

Figure 17 On the left, comparison between the three models (optimized systems with Hagnesia generators and IEA baseline) of the Power Spectral Density (PSD) of nacelle fore-aft acceleration (Nac TAx), tower top deflection in x direction (TWRTopXDef), wave elevation (WaveElev), platform pitch (PltfmPitch) and aerodynamic thrust (AeroThrust). On the right, the corresponding time series is shown. All the plots refer to a mean wind speed of 23 m/s in DLC1.6.

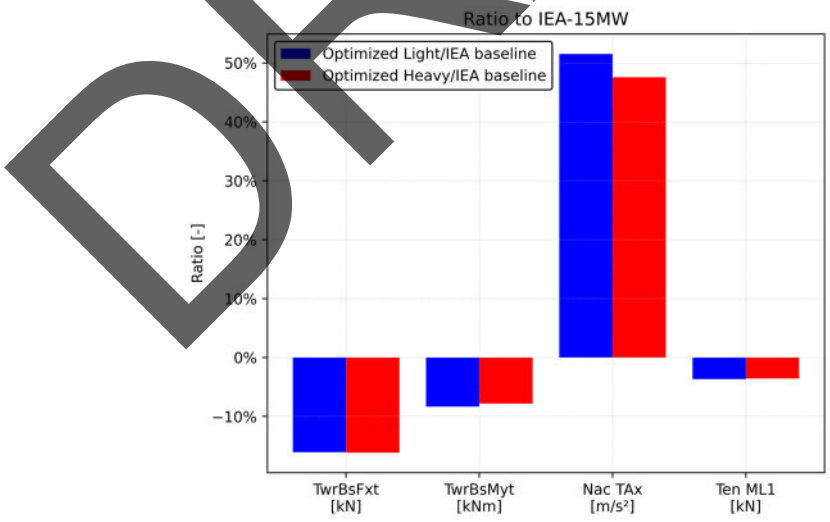

Figure 18 In red, the ratio (expressed as a relative percentage) of mean extreme load values for the optimized system with the heavy Hagnesia generator to that of the baseline IEA-15MW turbine. In blue, the same ratio for the optimized system with the light Hagnesia generator, relative to the baseline.

The ratio of ultimate loads measured with the optimized designs with respect to those recorded with the reference design are shown in Figure 18. In all the main load sensors reported, a reduction in the mean of maxima values is observed, except for the nacelle acceleration in the x-axis direction, which increases compared to what is shown in Figure 12. From this figure, it can be observed that a greater load reduction can be achieved through tower mass optimization and the drop-in replacement Hagnesia generators, with an improvement of more than 5% in the tower base fore-aft force. It is worth noticing that the lightweight tower designs, made possible by the reduction in RNA weight, satisfy the imposed maximum stress limits. Therefore, from the standpoint of natural frequencies and maximum stresses, the design is considered feasible according to this computational model. The load reduction may affect downstream components, such as the floater, which were not evaluated in this study. Fatigue loading limits were not included among the optimization constraints, so any reduction in damage equivalent loads would be a positive outcome.

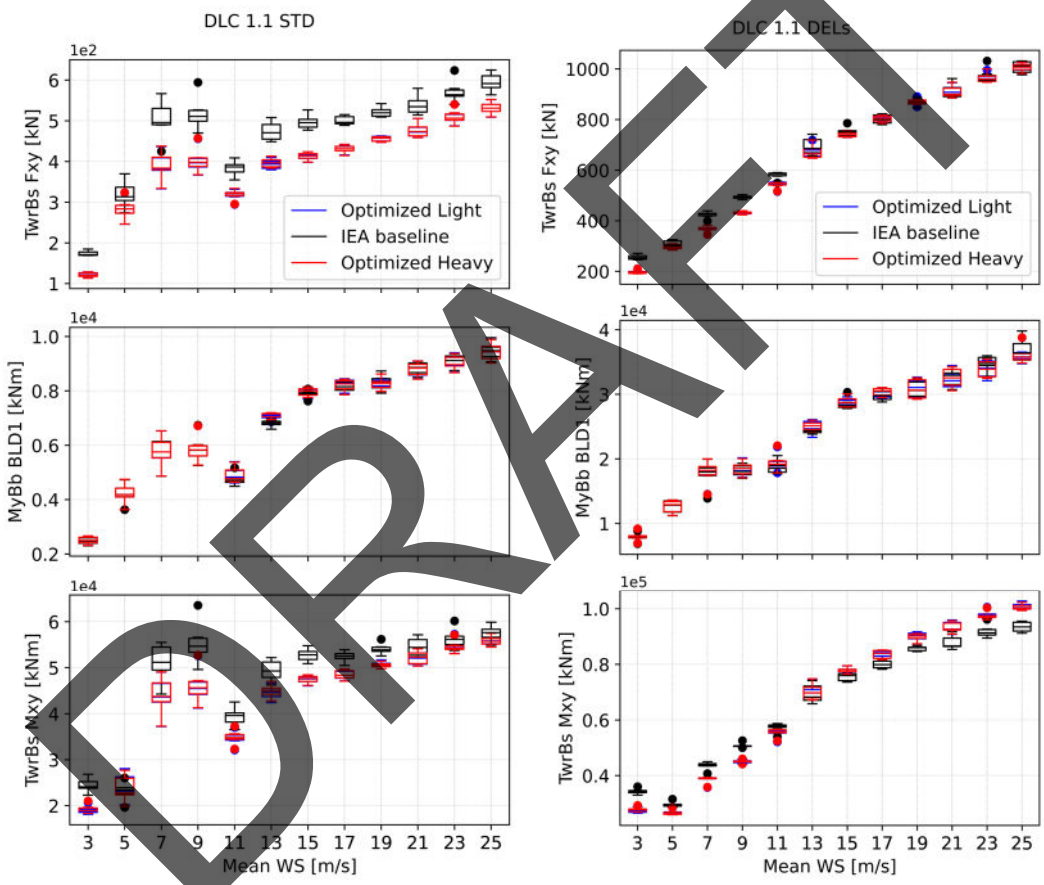

Figure 19 On the left, box plots of the standard deviation of the tower base force in the xy-plane (TwrBs Fxy), blade root bending moment in the y-direction (MyBb BLD1), and tower base bending moment in the xy-plane (TwrBs Mxy) are shown. On the right, 1-Hz zero mean DELs are plotted as a function of mean wind speed. Three cases are compared: the IEA baseline, and systems optimized with lighter (Optimized Light) and heavier (Optimized Heavy) generators. In this plot, the solid line within each box represents the median; boxes indicate the first and third quartiles, and the whiskers correspond to the 5th and 95th percentiles based on the six seeds simulated for each mean wind speed value.

Figure 19 shows DELs calculated for the two optimized systems compared to the baseline IEA-15MW RWT. DELs are calculated as explained in Section 3.3.3. By comparing Figure 19 with Figure 13 it is possible to notice that the obtained DELs in the optimized systems (Optimized Light and Optimized Heavy) are slightly higher than what is obtained for IEA-15MW with the Hagnesia generator designs. This may be attributed to a greater nacelle acceleration in these systems, as shown in Figure 16,

which results from the lower stiffness of the tower itself. This, in turn, causes additional varying inertial loads. However, as shown in Figure 20, the standard deviation is higher for the IEA-15MW baseline, indicating that the load amplitude is lower for the two optimized systems. Therefore, the increase in the Damage Equivalent Loads (DELs) may be a consequence of a higher number of load cycles in the simulation, leading to an increased frequency of these loads.

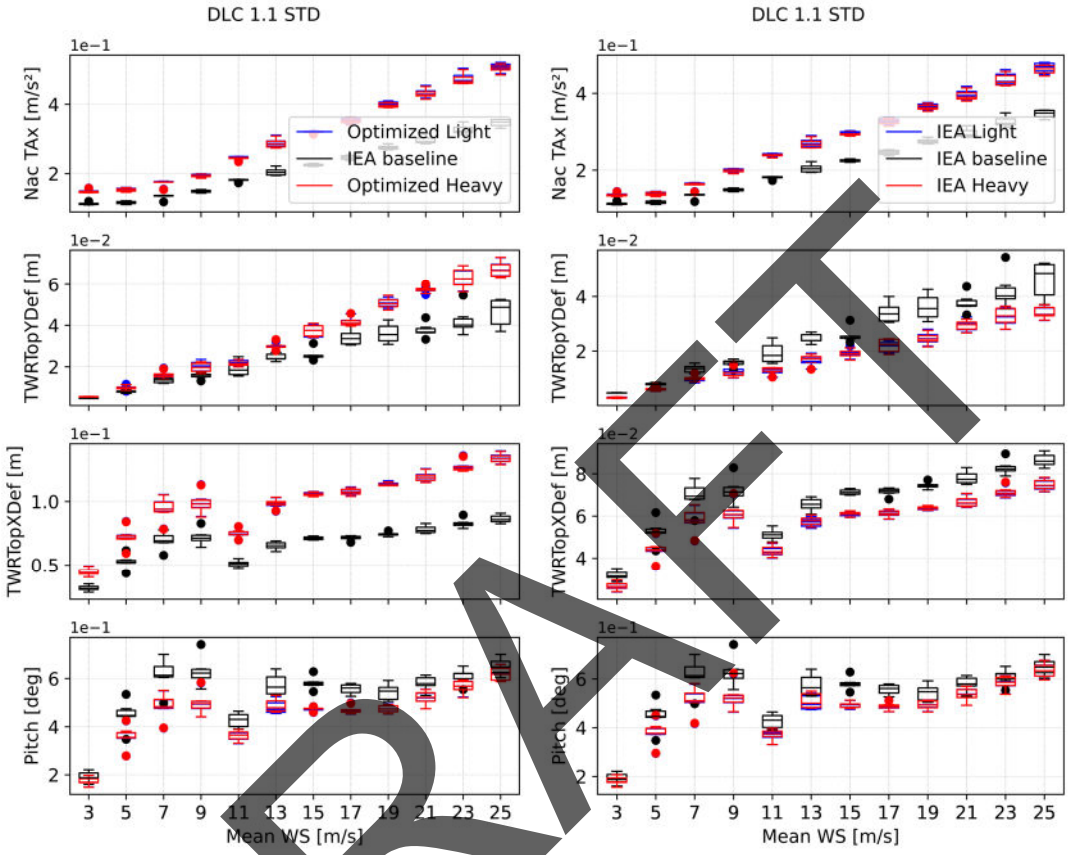

Figure 20 Box plots of the standard deviation of the fore-aft nacelle acceleration (Nac TAx), tower top displacement in the y-direction (TWRTopYDef), tower top displacement in the x-direction (TWRTopXDef), and platform pitch (Pitch) are shown.

Indeed, in both optimized systems, the tower is more flexible than in the baseline model. This is also confirmed by Table 7, where the first natural frequency of the tower is lower compared to that of the baseline model.

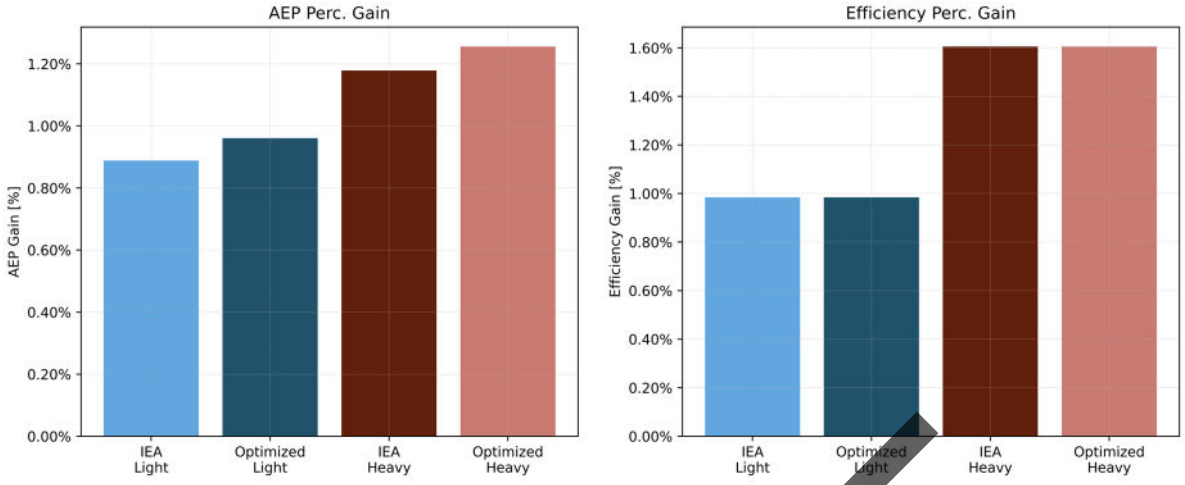

Figure 21 On the left percentage gain of Annual Energy Production (AEP) of all four systems analyzed with respect to the baseline IEA-15MW. The AEP percentage gain is calculated from electrical power. On the right, the efficiency gain of the Hagnesia generators compared to the IEA-15MW direct drive gearless generator.

A final comparison of all systems is conducted based on annual energy production which is calculated as in DLC1.1 as follows:

$$AEP = \sum_{i=1}^{N} \left(Power_{[i]} \cdot Probability_{[i]}\right) \cdot YearHours$$

where N denotes the total number of bins into which the Weibull distribution of wind speeds is divided, $YearHours$ represents the total number of hours in a year (8760) and the $Probability_{[i]}$ is the probability that the mean wind speed falls within the i_{th} bin. The annual energy production is calculated based on a Class 1 [48] Weibull distribution, characterized by a mean wind speed of 10 m/s and a shape factor of 2 (Rayleigh distribution). Values of the obtained AEP are presented in Table 9. Figure 21 presents the results obtained for the AEP. More specifically, the left side of Figure 21 shows the AEP gain relative to the IEA-15MW baseline, calculated using electrical power. The IEA Light and Optimized Light configurations use the same generator as the IEA Heavy and Optimized Heavy, respectively. The only difference between the optimized systems (both light and heavy) and IEA configurations lies in the tower design: in the Optimized Light and Optimized Heavy cases, the tower is optimized as described in Section 3.4, which leads to differences in the system's dynamic properties. To further investigate whether these dynamic differences can significantly impact the Annual Energy Production (AEP), the right side of Figure 21 also presents the trend in generator efficiency improvement associated with the Hagnesia generator concept. As reported in Table 2 and Table 5, the Hagnesia generator exhibits higher efficiency. Accordingly, as shown in Figure 21, the generator efficiency is the same for IEA Light and Optimized Light, as well as for IEA Heavy and Optimized Heavy, since the generator remains unchanged in each pair. In particular, the highest efficiency is achieved with the heavier generator, while the lighter configuration has a slightly lower efficiency, yet still higher than that of the baseline direct-drive generator used in the reference IEA-15MW turbine. The use of Hagnesia generators results in an AEP increase of up to 1% with the lighter configuration and up to 1.2% with the heavier one, potentially contributing to a reduction in the Levelized Cost of Energy (LCOE).

Table 9 Annual Energy Production in GWh

	IEA Light	Optimized Light	IEA Heavy	Optimized Heavy	IEA baseline
AEP [GWh]	81.448	81.506	81.682	81.745	80.730

Figure 21 clearly shows that AEP gains are consistent with the improvements in generator efficiency reported on the right side of the figure. Overall, this final comparison confirms that the trend in generator efficiency gain is directly reflected in the behavior of AEP. A breakdown of the energy output gains per wind speed bin is shown in Figure 22. Improvements in energy production are indeed noted only below rated wind speed. The amount of energy produced at each wind speed is proportional to the generator efficiency and the probability of each wind speed bin, determined based on the assumed long-term Rayleigh wind speed distribution. All three generator designs net the same energy production above 12 m/s wind speed.

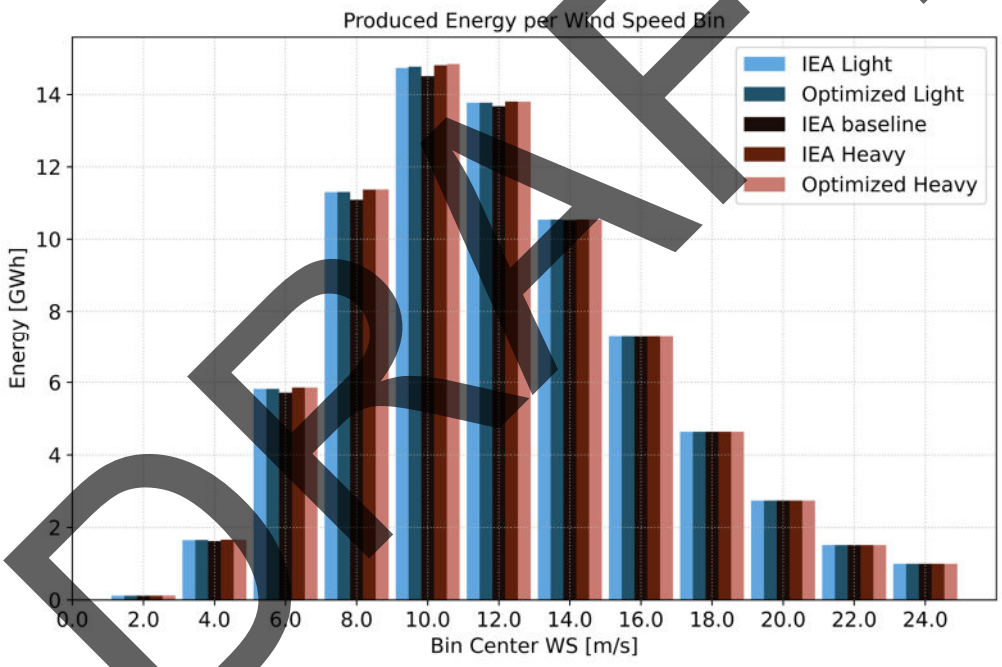

Figure 22 Obtained AEP for each Wind Speed bin.

3.5. Discussion and conclusion

A final comprehensive assessment of the resulting designs can now be presented. Aero-servo-hydro-elastic simulations, conducted using met-ocean conditions derived from the FLOATECH project, showed that replacing the baseline generator with the lighter Hagnesia designs led to a reduction in mean load values and mean maxima of ultimate loads, particularly the fore-aft tower base bending moment (TwrBsMyt). The reduction in this load sensor can ultimately be attributed to the decreased mass at the top of the tower. Mooring line tension was only marginally affected by generator weight. In the two optimized systems, the load reduction became even more significant, due to the combined

effect of reduced generator and tower mass and diameter, leading to lower gravitational and inertial loads. This optimization resulted in an improvement of over 5% in the tower base fore-aft shear force with respect to designs using the Hagnesia generator and reference tower, and a 10% reduction with respect to the baseline reference IEA 15MW design. However, it was observed that systems using the Hagnesia generators, both with and without tower optimization, exhibited significantly higher nacelle acceleration in the x-direction compared to the baseline IEA-15MW. From a general standpoint, this behavior is a result of increased pitch motion of the platform coupled with higher tower flexibility in the optimized designs. However, upon detailed examination of the data, a more nuanced connection between nacelle acceleration, platform motion, and system characteristics was noted, and is discussed in more detail in the following paragraph. It is worth noting that an increase in nacelle acceleration is a drawback, as, for instance, it leads to higher inertial loads. However, systems with lightweight generators have a Rotor Nacelle Assembly (RNA) that is approximately 35% lighter, as detailed in the previous paragraph. This means that while inertial loads increase due to the higher acceleration, there is also a mitigating effect resulting from the reduced mass of the RNA cantilevered on the tower top. A preliminary evaluation of fatigue loads showed that reducing generator mass enhances fatigue loads alleviation at the tower base sensors. While the Damage Equivalent Loads (DELs) were slightly higher for the optimized systems compared to just replacing the generator, the standard deviation was lower for the optimized systems, indicating lower load amplitudes compared to the baseline. This behavior was attributed to a higher number of load cycles resulting from increased nacelle acceleration.

While examining the structural characteristics of the obtained systems, we can observe that the effective rotational inertia of the entire turbine, including the substructure, in the pitch direction of both Optimized configuration (Section 3.4) and of the IEA-Light and IEA-Heavy (Section 3.3.3) reference systems, is reduced when Hagnesia generators are employed. This reduction is attributed to the concentration of mass closer to the overall center of gravity of the wind turbine system. In fact, water ballast in the substructure – much closer to the system's center of gravity - compensates for the reduction in generator mass. An additional critical factor is the vertical position of the center of gravity itself. As indicated in Table 8, the systems incorporating Hagnesia generators exhibit a lower center of gravity, with the lowest values observed in the two optimized configurations (Optimized Heavy and Optimized Light). This downward shift in the center of gravity positively influences the dynamic behavior of the floating platform. Specifically, the restoring forces, which are responsible for returning the structure to equilibrium following perturbations, are enhanced. These forces are partly dependent on the azimuthal positioning of the center of gravity; as the vertical (z-axis) coordinate of the center of gravity decreases, the restoring moment increases, thereby improving the system's dynamic stability. Additional details regarding the center of gravity positioning are provided in Table 8. A lower rotational inertia can result in higher accelerations under external loading conditions, such as wind and wave forces. Conversely, a reduction in the vertical position of the center of gravity increases the restoring force, as previously discussed. Referring to Figure 11 and Figure 17, which present the power spectral density (PSD) of the most relevant load sensors, it can be assumed that the increased restoring forces do not fully compensate for the reduced rotational inertia. This imbalance results in greater acceleration and displacement magnitudes. Another contributing factor is the increased flexibility of the tower in the Optimized configurations. As shown in Figure 17, the out-of-plane displacement at the tower top is greater than that of the IEA-15MW baseline. This behavior is attributed to the reduced stiffness of the tower structure. A similar trend is observed in Figure 20, which presents the fore-aft and side-to-side

deflections at the tower top. On the left-hand side of the figure, the tower top displacements in the two optimized models are higher than those of the IEA-15MW baseline, which has the original, stiffer tower configuration. It is important to note that restoring forces only act when there is a deviation from the equilibrium position. This leads to the following observation: when perturbed, the optimized system experiences higher acceleration compared to the baseline but simultaneously generates a greater restoring force. As a result, the standard deviation of pitch motion (Figure 20) is lower than that of the baseline configuration, meaning that these systems are less likely to tilt and move.

Additional considerations can be made regarding the annual energy production gains. As previously noted, AEP increases less if compared to the improvement in generator efficiency. This discrepancy is motivated by the fact that wind turbines operate in power-regulation mode at wind speeds above the rated value, commonly referred to as Region 3, where generator efficiency is no longer a factor, as the system actively regulates power output. For this reason, an improvement in generator efficiency can lead to an increase in AEP only in the below-rated region as shown in Figure 22. Nevertheless, AEP improvements of up to 1.2% are noted using the Hagnesia concept designs.

Regarding the generator design considerations, as discussed in Sections 3.3.3 and 3.4, the weight of the Hagnesia generators has a negligible impact on both overall turbine performance and tower design. In the baseline case, the generator accounts for only 1.9% of the total system weight, whereas with the use of Hagnesia generators, this percentage goes from 0.077% to 0.15% (Table 8). As further detailed in Section 3.4, a 15-ton variation in generator mass, corresponding to the difference between the two generator designs proposed by Hagnesia, does not significantly influence the tower configuration. The resulting tower structures are comparable from both structural and dynamic perspectives, as shown in Table 7. Furthermore, Table 8 indicates that the generator's moment of inertia also has a minimal effect, accounting for only 0.6% of the total rotor inertia in the baseline case and from 0.0327% to the 0.0472% for Hagnesia designs. These findings confirm that minor variations in generator mass and inertia, such as those found between the "light" and "heavy" variants of the Hagnesia generators, do not substantially impact the structural or dynamic behavior of the turbine. In addition, generator inertia contributes to overall rotor inertia in a minor way even in the case of the reference generator design and is therefore found to not be a design-driving parameter for the generator. Finally, the minor differences in system dynamics that were noted between the two generator designs suggest that for generators this light, system dynamics can be excluded from the design process, which can consider the generator alone. For instance, in this study, the increase in efficiency afforded by the heavier variant of the generator designs should be balanced only against the increase in cost of the generator itself, as other turbine components such as the tower and blades have been found to be mostly unaffected by the change in weight and inertia.

4. Conclusions

Floating Offshore Wind Turbines (FOWTs) present unique challenges compared to fixed-bottom offshore wind turbines, primarily due to the coupled dynamics of the wind turbine, floating platform, mooring system, and the marine environment. This document, Deliverable D1.1 of the European Union-funded FLOATFARM project (Grant Agreement N° 101136091), contributes to Work Package 1 (WP1) which aims to advance innovative technologies tailored for FOWTs to improve overall performance, reduce material usage, and ultimately lower the Levelized Cost of Energy (LCOE).

Specifically, this report focuses on Task 1.2, the objectives of which are twofold; firstly, a 15MW-scale concept lightweight generator design is outlined, and secondly the potential structural load reductions and raw material savings enabled by the novel, lightweight, gearless generator technology developed by Hagnesia are shown. A selection of possible design configurations are shown to illustrate the design space available and what impact different design choices will have on key performance indicators. While several unknowns concerning drivetrain integration and design loads will cause significant uncertainty in the estimated mass of the generator, it is shown that the potential wight savings are well above 90%. To evaluate potential impact on turbine design, a light and a heavy design configuration (which also differ correspondingly in efficiency and inertia) is proposed for turbine impact studies. The two configurations are selected in order to i) provide a preliminary sensitivity analysis on the influence of parameters such as generator inertia and mass on turbine performance; ii) evaluate the impact of generator load reduction in the presence of mass-estimation uncertainties. The generator weight is a critical factor in FOWTs as it is located high above sea level and imposes significant gravitational and inertial loads on the tower and substructure. Hagnesia's gearless direct-drive generator concept offers a substantial reduction in nacelle weight, with both the lighter (15 t) and heavier (30 t) designs being over ten times lighter than the 370-ton generator in the original IEA-15MW baseline model. The study employed the WEIS framework coupled with QBlade to evaluate the benefits of this technology. A key part of the work involved redesigning the tower of the IEA-15MW Reference Wind Turbine (RWT), replacing its original generator with the Hagnesia concept, to assess potential weight and load reductions. This optimization process focused on minimizing tower mass by changing tower diameter and layer thickness. The results demonstrate that utilizing the Hagnesia generator allows for a significant reduction in tower mass, achieving up to 30% material saving compared to the baseline tuned model of the IEA-15MW. The resulting designs are compliant with the reference turbine design in terms of tower natural frequencies, ultimate loading stresses and buckling limits. Aero-servo-hydro-elastic simulations, conducted using met-ocean conditions derived from the FLOATECH project, showed that replacing the baseline generator with the lighter Hagnesia designs led to a reduction in mean load values and mean maxima of ultimate loads, particularly the tower base bending moment (TwrBsMyt), attributed to the decreased mass at the top of the tower. In the two optimized systems, the load reduction became even more significant, due to the combined effect of reduced generator and tower mass and diameter, leading to lower gravitational and inertial loads. In addition, this optimization resulted in an improvement of over 5% in the tower base fore-aft force maximum value. However, it was observed that systems using the Hagnesia generators, both with and without tower optimization, exhibited significantly higher nacelle acceleration in the x-direction compared to the baseline IEA-15MW as a result of increased pitch motion of the platform coupled with higher tower flexibility in the optimized designs. A preliminary evaluation of fatigue loads showed that reducing generator also lowers fatigue loads alleviation at the tower base. However, Damage Equivalent Loads (DELs) were slightly higher for the optimized systems compared to just replacing the generator because of the highly coupled dynamic behaviour of FOWTs. As a matter of fact, optimizing a single component, such as the tower, in an isolated way may lead to worse overall system performance. While improvements to an individual subsystem may yield benefits from a single perspective, they can simultaneously degrade the performance of other subsystems. This is a consequence of the complex, non-linear interactions inherent in system dynamics. Nevertheless, the standard deviation was lower for the optimized systems, indicating lower load amplitudes compared to the baseline. While the resulting reduction in fatigue loads is a positive preliminary indication, more attention should be paid

to this aspect in future studies, as a detailed structural fatigue verification of the tower was not performed at this stage.

This study did not investigate potential weight savings in other wind turbine components. For instance, weight savings in the nacelle were not investigated, but could be expected due to the reduction in rotor-nacelle-assembly mass. In addition, the floating substructure design and mooring cable layout are assumed to be unchanged in this study. In fact, floater structural mass in academic reference designs such as the IEA 15MW RWT is estimated roughly. A detailed estimation of floater mass would require an equally detailed substructure design, including features such as internal baffles and reinforcements within the floater structure, which are generally neglected in the state-of-the-art engineering models that are used herein. Indeed, reaching such level of detail is currently possible only with higher-order design tools, generally based on Finite Element (FEA) and Computer-Assisted Desing (CAD) tools, which are only used in final design stages and not at a conceptual design phase. Nevertheless, altering the floater shape and the wind turbine controller tuning, both of which have been designed with the reference RNA weight in mind, could benefit system dynamics and afford further load reduction or mass reductions with respect to what has been shown herein. Future work on the topic should explore such aspects.

In conclusion, the adoption of the lightweight Hagnesia generator technology, coupled with tower optimization, offers significant benefits for FOWTs. Decreasing generator mass has shown promising potential in further material savings in components such as the tower. These factors positively impact the LCOE and contribute to advancing the next generation of environmentally friendly floating wind farms.

References

[1] Abbas, N. J., dzalkind, Barter, G., Bortolotti, P., Jasa, J., Mudafort, R. M., Nunemaker, J., paulf81, Chetan, M., Quon, E., Ramos, D. S., Liao, Y., Frontin, C., Lee, Y. H., Sundarrajan, A. K., Gaertner, E., Ryu, S., Branlard, E., Mulders, S., Gupta, A., Key, A., Heffernan, D., Motes, G., Rinker, J., Meunier, P.-E., Du, X., and amoratoc, 2025, "WISDEM/WEIS: V1.5.2 Release." https://doi.org/10.5281/zenodo.15133488.

[2] Abbas, N. J., dzalkind, Barter, G., Jasa, J., Bortolotti, P., Mudafort, R. M., Nunemaker, J., paulf81, rbehrensdeluna, Chetan, M., Quon, E., Ramos, D. S., Liao, Y., Lee, Y. H., Frontin, C., Sundarrajan, A. K., Gaertner, E., Branlard, E., Mulders, S., Key, A., Heffernan, D., Motes, G., Rinker, J., Meunier, P.-E., Du, X., and amoratoc, 2025, "Rbehrensdeluna/QBtoWEIS: QBtoWEIS v1.0.0." https://doi.org/10.5281/zenodo.14754213.

[3] Carrara, S., Baldassarre, B., Jakimów, M., Kuzov, T., Mc Govern, L., Nohl, L., Ierides, M., and Christou, M., 2025, *Deep Dive on Critical Raw Materials for Wind Turbines in the EU*, Publications Office of the European Union. [Online]. Available: https://data.europa.eu/doi/10.2760/5665594. [Accessed: 10-Jun-2025].

[4] Sethuraman, L., and Dykes, K. L., 2017, *GeneratorSE: A Sizing Tool for Variable-Speed Wind Turbine Generators*, NREL/TP--5000-66462, 1395455. https://doi.org/10.2172/1395455.

[5] "Magnax - Yokeless Axial Flux Technology," Magnax - Yokeless Axial Flux Technol. [Online]. Available: https://www.magnax.com. [Accessed: 20-Jun-2025].

[6] actadmin, "Home," GreenSpur Wind. [Online]. Available: https://www.greenspur.co.uk/. [Accessed: 03-Jun-2025].

[7] Bang, D., Polinder, H., Shrestha, G., and Ferreira, J. A., 2009, "Ring-Shaped Transverse Flux PM Generator for Large Direct-Drive Wind Turbines," *2009 International Conference on Power Electronics and Drive Systems (PEDS)*, pp. 61–66. https://doi.org/10.1109/PEDS.2009.5385933.

[8] Siatkowski, M., and Orlik, B., 2008, "Influence of Saturation Effects in a Transverse Flux Machine," *2008 13th International Power Electronics and Motion Control Conference*, pp. 830–836. https://doi.org/10.1109/EPEPEMC.2008.4635370.

[9] "Pseudo Direct Drive," Magnomatics. [Online]. Available: https://www.magnomatics.com/pseudo-direct-drive. [Accessed: 03-Jun-2025].

[10] Penzkofer, A., and Atallah, K., 2016, "Scaling of Pseudo Direct Drives for Wind Turbine Application," IEEE Trans. Magn., 52(7), pp. 1–5. https://doi.org/10.1109/TMAG.2016.2524205.

[11] Winkler, T., and Consortium, on behalf of the E., 2019, "The EcoSwing Project," IOP Conf. Ser. Mater. Sci. Eng., 502(1), p. 012004. https://doi.org/10.1088/1757-899X/502/1/012004.

[12] Nordelöf, A., 2024, "Environmental Assessment of a Novel Generator Design in a 15 MW Wind Turbine." [Online]. Available: https://research.chalmers.se/en/publication/543783. [Accessed: 10-Jun-2025].

[13] HAGNESTÅL, A., and KEIJSER, M., 2022, "An Electrical Machine with an Isolated Rotor." [Online]. Available: https://patents.google.com/patent/WO2022050888A1/en?oq=WO2022050888A1. [Accessed: 11-Jun-2025].

[14] Hagnestål, A., 2023, "Azimuthal or Polodial Flux Machines." [Online]. Available: https://patents.google.com/patent/US11728717B2/en?oq=US11728717B2%2c. [Accessed: 11-Jun-2025].

[15] HAGNESTÅL, A., and KEIJSER, M., 2022, "Electrical Flux-Switching Machine with Structural Support." [Online]. Available: https://patents.google.com/patent/WO2022050887A1/en?oq=WO2022050887A1. [Accessed: 11-Jun-2025].

[16] Hagnestål, A., and KEIJSER, M., 2023, "Winding Arrangement for Modulated Pole Machines." [Online]. Available: https://patents.google.com/patent/US20230268815A1/en. [Accessed: 11-Jun-2025].

[17] "NextGen – Hagnesia." [Online]. Available: https://hagnesia.com/projects/nextgen/. [Accessed: 03-Jun-2025].

[18] Gaertner, E., Rinker, J., Sethuraman, L., Zahle, F., Anderson, B., Barter, G., Abbas, N., Meng, F., Bortolotti, P., Skrzypinski, W., Scott, G., Feil, R., Bredmose, H., Dykes, K., Shields, M., Allen, C., and Viselli, A., "Definition of the IEA 15-Megawatt Offshore Reference Wind."

[19] Barter, G. E., Sethuraman, L., Bortolotti, P., Keller, J., and Torrey, D. A., 2023, "Beyond 15 MW: A Cost of Energy Perspective on the next Generation of Drivetrain Technologies for Offshore Wind Turbines," Appl. Energy, 344, p. 121272. https://doi.org/10.1016/j.apenergy.2023.121272.

[20] Zahle, F., Barlas, A., Loenbaek, K., Bortolotti, P., Zalkind, D., Wang, L., Labuschagne, C., Sethuraman, L., and Barter, G., 2024, *Definition of the IEA Wind 22-Megawatt Offshore Reference Wind Turbine*, Technical University of Denmark. https://doi.org/10.11581/DTU.00000317.

[21] Allen, C., Viscelli, A., Dagher, H., Goupee, A., Gaertner, E., Abbas, N., Hall, M., and Barter, G., 2020, *Definition of the UMaine VolturnUS-S Reference Platform Developed for the IEA Wind 15-Megawatt Offshore Reference Wind Turbine*, NREL/TP--5000-76773, 1660012, MainId:9434. https://doi.org/10.2172/1660012.

[22] Bortolotti, P., Mudafort, R. M., Bay, C., kenloen, Quick, J., Barter, G., dzalkind, Zahle, F., amirarasteh1990, Lejeune, M., and madsmpedersen, 2025, "IEAWindSystems/windIO: Trigger Zenodo." https://doi.org/10.5281/zenodo.15191297.

[23] Barter, G., Bortolotti, P., Gaertner, E., Rinker, J., Abbas, N. J., dzalkind, Zahle, F., T-Wainwright, Branlard, E., Wang, L., Padrón, L. A., Hall, M., and lssraman, 2024, "IEAWindTask37/IEA-15-240-RWT: V1.1.10: Correct Errors in OpenFAST Monopile SubDyn Module." https://doi.org/10.5281/zenodo.10664562.

[24] "QBlade v2.0.4 Documentation," ResearchGate. [Online]. Available: https://www.researchgate.net/publication/362720536_QBlade_v204_Documentation. [Accessed: 12-May-2025].

[25] Allen, C., Viscelli, A., Dagher, H., Goupee, A., Gaertner, E., Abbas, N., Hall, M., and Barter, G., 2020, *Definition of the UMaine VolturnUS-S Reference Platform Developed for the IEA Wind 15-Megawatt Offshore Reference Wind Turbine*, NREL/TP--5000-76773, 1660012, MainId:9434. https://doi.org/10.2172/1660012.

[26] Bortolotti, P., Mudafort, R. M., Bay, C., kenloen, Quick, J., Barter, G., dzalkind, Zahle, F., amirarasteh1990, Lejeune, M., and madsmpedersen, 2025, "IEAWindSystems/windIO." https://doi.org/10.5281/zenodo.15191297.

[27] Gray, J. S., Hwang, J. T., Martins, J. R. R. A., Moore, K. T., and Naylor, B. A., 2019, "OpenMDAO: An Open-Source Framework for Multidisciplinary Design, Analysis, and Optimization," Struct. Multidiscip. Optim., 59(4), pp. 1075–1104. https://doi.org/10.1007/s00158-019-02211-z.

[28] Abbas, N., Jasa, J., Zalkind, D., Wright, A., and Pao, L., 2024, "Control Co-Design of a Floating Offshore Wind Turbine: Article No. 122036," Appl. Energy, 353(Part B). https://doi.org/10.1016/j.apenergy.2023.122036.

[29] Pao, L. Y., Pusch, M., and Zalkind, D. S., 2024, "Control Co-Design of Wind Turbines," Annu. Rev. Control Robot. Auton. Syst., 7(Volume 7, 2024), pp. 201–226. https://doi.org/10.1146/annurev-control-061423-101708.

[30] Powell, M. J. D., 1994, "A Direct Search Optimization Method That Models the Objective and Constraint Functions by Linear Interpolation," *Advances in Optimization and Numerical Analysis*, S. Gomez, and J.-P. Hennart, eds., Springer Netherlands, Dordrecht, pp. 51–67. https://doi.org/10.1007/978-94-015-8330-5_4.

[31] "OpenFAST Documentation — OpenFAST v4.0.2 Documentation." [Online]. Available: https://openfast.readthedocs.io/en/main/. [Accessed: 18-Apr-2025].

[32] Hall, M., Housner, S., Zalkind, D., Bortolotti, P., Ogden, D., and Barter, G., 2022, "An Open-Source Frequency-Domain Model for Floating Wind Turbine Design Optimization," J. Phys. Conf. Ser., 2265(4), p. 042020. https://doi.org/10.1088/1742-6596/2265/4/042020.

[33] Behrens de Luna, R., 2025, "QBlade Interfacing Framework." [Online]. Available: https://zenodo.org/records/15623707. [Accessed: 19-Jun-2025].

[34] "Wamit, Inc. - The State of the Art in Wave Interaction Analysis." [Online]. Available: https://www.wamit.com/manualv7.4/wamit_v74manual.html. [Accessed: 29-Apr-2025].

[35] Faltinsen, O., 1993, *Sea Loads on Ships and Offshore Structures*, Cambridge University Press.

[36] Bonnefoy, F., Delacroix, S., Ducrozet, G., Kim, I., and Leroy, V., 2023, "FLOATECH WP3 Experimental Wave Database." https://doi.org/10.5281/zenodo.7689781.

[37] 2005, "Wind Turbines - Part 1: Design Requirements."

[38] "IEC 61400-3-1:2019." [Online]. Available: https://webstore.iec.ch/en/publication/29360. [Accessed: 30-Apr-2025].

[39] "Design Load Analysis of Two Floating Offshore Wind Turbine Concepts." [Online]. Available: https://scholarworks.umass.edu/entities/publication/ab8babce-3694-4a6c-8cf3-0ee50f8d87f2. [Accessed: 05-May-2025].

[40] Buhl, M., "MCrunch User's Guide."

[41] Madsen, H. A., Larsen, T. J., Pirrung, G. R., Li, A., and Zahle, F., 2020, "Implementation of the Blade Element Momentum Model on a Polar Grid and Its Aeroelastic Load Impact," Wind Energy Sci., 5(1), pp. 1–27. https://doi.org/10.5194/wes-5-1-2020.

[42] Tasora, A., Serban, R., Mazhar, H., Pazouki, A., Melanz, D., Fleischmann, J., Taylor, M., Sugiyama, H., and Negrut, D., 2016, "Chrono: An Open Source Multi-Physics Dynamics Engine," *High Performance Computing in Science and Engineering*, T. Kozubek, R. Blaheta, J. Šístek, M. Rozložník, and M. Čermák, eds., Springer International Publishing, Cham, pp. 19–49. https://doi.org/10.1007/978-3-319-40361-8_2.

[43] Marten, D., 2020, "QBlade: A Modern Tool for the Aeroelastic Simulation of Wind Turbines." [Online]. Available: https://depositonce.tu-berlin.de/handle/11303/11758. [Accessed: 19-May-2025].

[44] Abbas, N. J., Zalkind, D. S., Pao, L., and Wright, A., 2022, "A Reference Open-Source Controller for Fixed and Floating Offshore Wind Turbines," Wind Energy Sci., 7(1), pp. 53–73. https://doi.org/10.5194/wes-7-53-2022.

[45] Larsen, T. J., and Hanson, T. D., 2007, "A Method to Avoid Negative Damped Low Frequent Tower Vibrations for a Floating, Pitch Controlled Wind Turbine," J. Phys. Conf. Ser., 75(1), p. 012073. https://doi.org/10.1088/1742-6596/75/1/012073.

[46] "IEA-15-240-RWT/OpenFAST/IEA-15-240-RWT-UMaineSemi/IEA-15-240-RWT-UMaineSemi_DISCON.IN at Master · IEAWindSystems/IEA-15-240-RWT." [Online]. Available: https://github.com/IEAWindSystems/IEA-15-240-RWT/blob/master/OpenFAST/IEA-15-240-RWT-UMaineSemi/IEA-15-240-RWT-UMaineSemi_DISCON.IN. [Accessed: 20-May-2025].

[47] Behrens de Luna, R., Perez-Becker, S., Saverin, J., Marten, D., Papi, F., Ducasse, M.-L., Bonnefoy, F., Bianchini, A., and Paschereit, C.-O., 2024, "Quantifying the Impact of Modeling Fidelity on Different Substructure Concepts for Floating Offshore Wind Turbines – Part 1: Validation of the Hydrodynamic Module QBlade-Ocean," Wind Energy Sci., 9(3), pp. 623–649. https://doi.org/10.5194/wes-9-623-2024.

[48] "IEC 61400-1:2019." [Online]. Available: https://webstore.iec.ch/en/publication/26423. [Accessed: 10-Jun-2025].

[49] Hayman, G. J., "MLife Theory Manual for Version 1.00."

[50] "Eurocode 3: Design of Steel Structures | Eurocodes: Building the Future." [Online]. Available: https://eurocodes.jrc.ec.europa.eu/EN-Eurocodes/eurocode-3-design-steel-structures. [Accessed: 09-May-2025].

[51] Pao, L. Y., Pusch, M., and Zalkind, D. S., 2024, "Control Co-Design of Wind Turbines," Annu. Rev. Control Robot. Auton. Syst., 7(1), pp. 201–226. https://doi.org/10.1146/annurev-control-061423-101708.